Received: 3 May 2023 | Revised: 18 August 2023 | Accepted: 21 August 2023

DOI: 10.1111/pce.14706

ORIGINAL ARTICLE

Plant, Cell & Environment | WILEY

Spermine deficiency shifts the balance between jasmonic acid and salicylic acid-mediated defence responses in *Arabidopsis*

Chi Zhang[1] | Kostadin E. Atanasov[1] | Ester Murillo[1] | Vicente Vives-Peris[2] | Jiaqi Zhao[1] | Cuiyun Deng[3] | Aurelio Gómez-Cadenas[2] | Rubén Alcázar[1]

[1]Department of Biology, Healthcare and Environment, Section of Plant Physiology, Faculty of Pharmacy and Food Sciences, Universitat de Barcelona, Barcelona, Spain

[2]Departamento de Biología, Bioquímica y Ciencias Naturales, Universitat Jaume I, Castelló de la Plana, Spain

[3]Plant Synthetic Biology and Metabolic Engineering Program, Centre for Research in Agricultural Genomics (CRAG), CSIC-IRTA-UAB-UB, Cerdanyola, Barcelona, Spain

Correspondence
Rubén Alcázar, Department of Biology, Healthcare and Environment, Section of Plant Physiology, Faculty of Pharmacy and Food Sciences, Universitat de Barcelona, Av. Joan XXIII 27-31, 08028 Barcelona, Spain.
Email: ralcazar@ub.edu

Funding information
Ministerio de Ciencia e Innovación MCIN/ Agencia Estatal de Investigación AEI/ 10.13039/501100011033 (Spain)

Abstract

Polyamines are small aliphatic polycations present in all living organisms. In plants, the most abundant polyamines are putrescine (Put), spermidine (Spd) and spermine (Spm). Polyamine levels change in response to different pathogens, including *Pseudomonas syringae* pv. *tomato* DC3000 (*Pst* DC3000). However, the regulation of polyamine metabolism and their specific contributions to defence are not fully understood. Here we report that stimulation of Put biosynthesis by *Pst* DC3000 is dependent on coronatine (COR) perception and jasmonic acid (JA) signalling, independently of salicylic acid (SA). Conversely, lack of Spm in *spermine synthase* (*spms*) mutant stimulated galactolipids and JA biosynthesis, and JA signalling under basal conditions and during *Pst* DC3000 infection, whereas compromised SA-pathway activation and defence outputs through SA–JA antagonism. The dampening of SA responses correlated with COR and *Pst* DC3000-inducible deregulation of *ANAC019* expression and its key SA-metabolism gene targets. Spm deficiency also led to enhanced disease resistance to the necrotrophic fungal pathogen *Botrytis cinerea* and stimulated endoplasmic reticulum (ER) stress signalling in response to *Pst* DC3000. Overall, our findings provide evidence for the integration of polyamine metabolism in JA- and SA-mediated defence responses, as well as the participation of Spm in buffering ER stress during defence.

KEYWORDS
Botrytis cinerea, coronatine, ER stress, galactolipids, JA, polyamines, *Pseudomonas syringae*, SA

1 | INTRODUCTION

Polyamines are aliphatic polycations of small molecular weight present in all living organisms. In plants, the major polyamines are putrescine (Put), spermidine (Spd) and spermine (Spm) (Figure 1a). Changes in polyamine metabolism are part of the metabolic reprogramming that takes place during the defence response of plants (Gerlin et al., 2021; Tiburcio et al., 2014). Exogenously supplied Put triggers the formation of callose deposits and the expression of PAMP (pathogen associated molecular pattern)-triggered immunity (PTI) marker genes, which are reliant on hydrogen peroxide (H_2O_2) production and NADPH oxidase function (Liu et al., 2019). Moreover, Put stimulates salicylic acid (SA) accumulation in local leaves and triggers local and systemic transcriptional reprogramming that

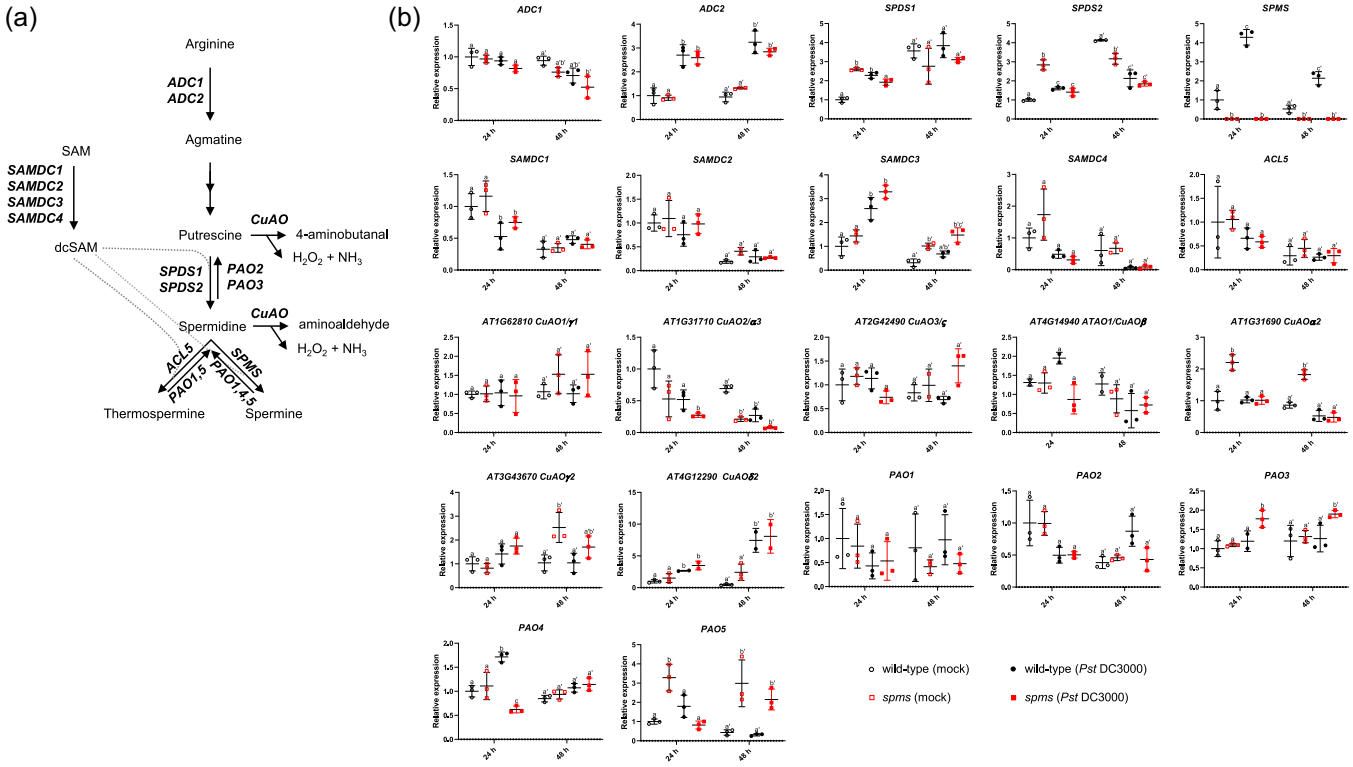

FIGURE 1 (a) Polyamine biosynthesis and oxidation in *Arabidopsis*. (b) Transcriptional changes of polyamine metabolism genes in response to *Pst* DC3000. Expression analyses of polyamine biosynthesis and oxidation genes in wild-type and *spermine synthase* (*spms*) plants at 24 and 48 h of *Pst* DC3000 and mock (10 mM $MgCl_2$) inoculation. Expression values are relative to wild-type (mock) treatment and represent the mean ± SD from three biological replicates per point of analysis. Different letters indicate significant differences ($p < 0.05$) according to two-way analysis of variance followed by Tukey's posthoc test. *ACL5* (*ACAULIS5*), thermospermine synthase; ADC, arginine decarboxylase; CuAO, copper-containing amine oxidase; dcSAM, decarboxylated SAM; PAO, polyamine oxidase; SAM, S-adenosylmethionine; SAMDC, S-adenosylmethionine decarboxylase; SPDS, spermidine synthase; SPMS, spermine synthase.

partially overlap with the systemic acquired resistance (SAR) response (Liu et al., 2020a). The transcriptional changes elicited by Put are partially compromised in *eds1-2*, *sid2-1* and *npr1-1* mutants, thus highlighting the importance of the SA-pathway in Put responses (Liu et al., 2020a).

The oxidation of Spm via polyamine oxidase (PAO) activity stimulates the activation of mitogen-activated protein kinases (MAPKs) (Seo et al., 2007; Zhang et al., 1997) and plays a crucial role in conditioning resistance to different pathogenic microorganisms such as *Pseudomonas syringae*, *Pseudomonas viridiflaba*, *Hyaloperonospora arabidopsidis*, *Verticillium dahlia*, *Botrytis cinerea* and cucumber mosaic virus (Gonzalez et al., 2011; Lou et al., 2016; Marco et al., 2014; Marina et al., 2008; Mitsuya et al., 2009; Mo et al., 2015; Moschou et al., 2009; Sagor et al., 2012). In tobacco, Spm induces the activation of protein kinases SA-induced protein kinase and wound-induced protein kinase, as well as MAPKs (Seo et al., 2007; Takahashi et al., 2003; Zhang et al., 1997). This activation leads to the expression of several hypersensitive response marker genes in a reactive oxygen species (ROS) and Ca^{2+}-dependent manner, independently of SA (Takahashi et al., 2004). Spm also inhibits PAMP-elicited RESPIRATORY BURST OXIDASE HOMOLOGUE D ROS production in a SA-independent manner, thus reshaping PTI responses (Zhang et al., 2023). Although there has been a substantial body of research conducted on the contribution of polyamines to defence, the precise mechanisms involved in this process are not yet fully understood. Specifically, the interaction between polyamines, SA and jasmonic acid (JA) pathways during defence deserved further investigation.

SA is an important plant defence hormone that provides immunity against biotrophic and semibiotrophic pathogens (Peng et al., 2021). In *Arabidopsis*, SA production during pathogen defence is primarily derived from the isochorismate synthase (ICS) pathway (Wildermuth et al., 2001). Mutations in *ICS1*, which are found in SA-deficient 2 (*sid2*) mutants, compromise SA accumulation (Garcion et al., 2008). SA biosynthesis also requires AvrPphB Susceptible 3 (PBS3), which catalyses the conjugation of isochorismate to glutamate, and ENHANCED DISEASE SUSCEPTIBILITY 5 (EDS5), which transports isochorismate to the cytosol (Nawrath et al., 2002; Serrano et al., 2013). *ICS1*, *PBS3*, and *EDS5* expression are strongly induced during the defence response and their transcription is coordinately regulated by the master regulators of plant immune responses SAR-DEFICIENT 1 (SARD1) and CALMODULIN-BINDING PROTEIN 60-LIKE g (CBP60g) (Sun et al., 2015; Wang et al., 2011; Zhang et al., 2010). Overexpression of *SARD1* is sufficient to activate *ICS1* expression, which points to a

regulation of SARD1 activity at transcriptional level (Zhang et al., 2010). ENHANCED DISEASE SUSCEPTIBILITY 1 (EDS1) and PHYTOALEXIN DEFICIENT 4 (PAD4) are also required for SA synthesis during effector-triggered immunity and basal defences (Dongus & Parker, 2021; Feys et al., 2001; Zhou et al., 1998).

SA is subject to multiple chemical modifications, including methylation and glycosylation. SALICYLIC ACID/BENZOIC ACID CARBOXYL METHYLTRANSFERASE (BSMT1) catalyses the production of the volatile methyl SA (Attaran et al., 2009). In addition, SALICYLIC ACID GLUCOSYLTRANSFERASE 1 (SAGT1) converts SA to its glucose ester (Dean & Delaney, 2008), thereby modulating the dynamics of SA homoeostasis and defence outputs (Zhang et al., 2010). SA is also a well-established signalling molecule for SAR. It is essential for the activation of genes involved in N-hydroxypipecolic acid biosynthesis, including *AGD2-LIKE DEFENCE RESPONSE PROTEIN 1* (*ALD1*), *SAR-DEFICIENT 4*, and *FLAVIN-DEPENDENT MONOOXYGENASE 1* (*FMO1*) (Liu et al., 2020b; Sun et al., 2020).

Although the promotion of disease resistance against biotrophic pathogens is attributed to SA, immunity against necrotrophic pathogens is associated with JA (Glazebrook, 2005). Jasmonates (JAs) are a type of lipid-derived signalling compound that are synthesized from α-linolenic acid (α-LeA) released from galactolipids (Ishiguro et al., 2001). α-LeA is a substrate of plastidial 13-Lipoxygenases (LOX2, LOX3, LOX4 and LOX6), which catalyse the synthesis of 13-hydroperoxy derivatives (Andreou & Feussner, 2009; Wasternack & Song, 2017). In turn, the 13-hydroperoxy derivatives are substrates of allene oxide synthase (AOS), a cytochrome P450 enzyme of the CYP74 family. The unstable allylic epoxides formed by AOS are converted into 12-oxophytodienoic acid (OPDA) by allene oxide cyclase (AOC), being the last reaction of the JA biosynthesis pathway in the chloroplast. Subsequently, the downstream steps in the biosynthesis of JA take place in the peroxisomes. OPDA is a substrate of OPDA reductase (OPR3) and this is followed by shortening of the carboxyl side chain by the fatty acid β-oxidation machinery (Hu et al., 2012; Wasternack & Song, 2017).

JA is conjugated to amino acids, such as isoleucine, and JA-Ile represents the major active jasmonate. JA is perceived by the JA receptor F-box protein CORONATINE INSENSITIVE1 (COI1) that forms a Skp-Cullin-F-box E3 ubiquitin ligase complex SCF (COI1) (Sheard et al., 2010; Wasternack & Feussner, 2018). JASMONATE ZIM DOMAIN (JAZ) proteins act as transcriptional repressors and function as co-receptors of JA perception (Chini et al., 2007; Sheard et al., 2010; Thines et al., 2007). When JA-Ile binds to COI1, it leads to the degradation of JAZ proteins through the 26S proteasome. This degradation removes the inhibitory effect of JAZ on the transcription factor MYC2 and its homologues, thus promoting the expression of genes that are responsive to JA signalling (Hou & Tsuda, 2022; Li et al., 2021).

Notably, SA and JA exhibit mutually antagonistic effects (Glazebrook, 2005). JA inhibits SA accumulation, as evidenced by the high levels of SA in JA-insensitive *coi1* and *myc2* mutants (Kloek et al., 2001; Nickstadt et al., 2004). The bacterial phytotoxin coronatine (COR), which is produced by various strains of *P. syringae* and exhibits structural similarity to JA-Ile (Mittal & Davis, 1995), facilitates bacterial growth and disease symptom development by stimulating the reopening of stomata and inhibiting SA accumulation (Brooks et al., 2005; Cui et al., 2005; Melotto et al., 2006; Mittal & Davis, 1995; Zheng et al., 2012). The *Arabidopsis ANAC019*, *ANAC055*, and *ANAC072*, which are homologous to NAC (NAM-ATAF1,2-CUC2) transcription factors, have been identified as key mediators of the COR-induced effects. Specifically, they contribute to *MYC2*-dependent inhibition of the SA pathway by suppressing *ICS1* and activating *BSMT1* expression, resulting in an overall reduction of SA (Zheng et al., 2012).

In this work, we investigated the involvement of the polyamine Spm in the defence response to *P. syringae* in *Arabidopsis*. We provide evidence that COR and JA signalling are important regulators of polyamine metabolism during the defence response to *P. syringae*. By performing RNA sequencing (RNA-seq) gene expression analyses in Spm-deficient mutant (*spms*) challenged with *Pst* DC3000, we find that Spm deficiency modifies the balance between JA and SA, and triggers endoplasmic reticulum (ER) stress responses. Through an untargeted lipidomics analysis, we demonstrate that Spm-deficient plants contain higher levels of monogalactosyldiacylglycerol (MGDG) and stimulate JA biosynthesis through expression regulation not involving increased peroxisomal β-oxidation. Spm deficiency dampens SA-mediated defences in correlation with the transcriptional upregulation of *ANAC019* and *BSMT1* expression, and *ICS1* downregulation. In contrast, Spm deficiency is found to enhance disease resistance to *B. cinerea* infection. Finally, Spm is shown to be critical for the mitigation of ER stress during the defence response to *P. syringae*. Overall, this work sheds new light on the integration of polyamines in the defence responses mediated by JA and SA, and in buffering ER stress signalling.

2 | MATERIALS AND METHODS

2.1 | Plant materials and growth conditions

Seeds of the different genotypes were directly sown on soil (40% peat moss, 50% vermiculite and 10% perlite). Seeds were stratified in the dark at 4°C for 2–3 days to stimulate germination. The different plant genotypes were grown at 20°C–22°C under 12 h light/12 h dark photoperiod cycles at 100–125 µmol photons m^{-2} s^{-1} of light intensity and 60%–70% relative humidity. The genotypes used in this work were in the Col-0 background: *spms* (Zhang et al., 2023), *eds1-2* (Feys et al., 2005), *sid2-1* (Wildermuth et al., 2001), *npr1-1* (Cao et al., 1997), *coi1-1* (Feys et al., 1994), *myc2* (Chini et al., 2007), *adc1* and *adc2* (Cuevas et al., 2008). For in vitro growth, seeds were sterilized in 30% sodium hypochlorite supplemented with 0.5% Triton X-100 (Merck) for 10 min, followed by three washes with sterile distilled H_2O. Seeds were sown on half-strength Murashige and Skoog (MS) medium (0.5× MS salts supplemented with vitamins [Duchefa Biochemie], 1% sucrose, 0.6% plant agar and 0.05% MES adjusted to pH 5.7 with 1 M KOH). To synchronize germination,

seeds were stratified in the dark at 4°C for 2–3 days. The seeds were kindly provided by Professor Jane Parker (*eds1-2*, *sid2-1*), Professor Xinnian Dong (*npr1-1*), Dr. Andrea Chini (*coi1-1*) or obtained from the Nottingham *Arabidopsis* Stock Centre (www.arabidopsis.info).

2.2 | Leaf infiltration and sampling

Infiltration of leaves with *Pst* DC3000 (OD_{600} = 0.001), *Pst* DC3000 Δ*cor* (OD_{600} = 0.001) (Ma et al., 1991) or mock (10 mM $MgCl_2$) was conducted on 5-week-old *Arabidopsis* plants using a 1 mL needleless syringe. The infiltration was performed on fully expanded rosette leaves using three leaves per plant, which represented one biological replicate. A minimum of three biological replicates were used in every analysis. Leaves at the same developmental stage were always chosen for infiltration of the different genotypes. At the indicated time points, only the infiltrated leaves were collected for the determination of polyamine levels, expression analyses (RNA-seq and quantitative reverse-transcription polymerase chain reaction [qRT-PCR]) and measurement of hormone levels (SA, JA, JA-Ile and OPDA). For the untargeted proteomics and lipidomics analyses, rosette leaves from untreated 5-week-old *spms* and wild-type plants were directly harvested using three leaves per plant as single biological replicate (n = 4 untargeted proteomics; n = 5 untargeted lipidomics). Leaves at the same developmental stage were always chosen for the analyses. The *Pst* DC3000 Δ*cor* strain was kindly provided by Professor Jane Parker.

2.3 | qRT-PCR gene expression analyses

Total RNA was extracted using TRIzol reagent (Thermo Fisher). Two micrograms of RNA were treated with DNAse I (Thermo Fisher) and first-strand complementary DNA (cDNA) synthesized using Superscript IV reverse transcriptase (Thermo Fisher) and oligo(dT) according to manufacturer's instructions. Quantitative real-time PCR using SYBR Green I dye method was performed on Roche LightCycler 480 II detector system following the PCR conditions: 95°C 2 min, 40 cycles (95°C, 15 s; 60°C, 30 s; 68°C, 20 s). To ensure comparable PCR efficiencies between the primer pairs used, standard curves were generated by performing serial dilutions of wild-type cDNA. The relative quantification was then determined using the $\Delta\Delta C_T$ method (Livak & Schmittgen, 2001). Gene expression was normalized using *ACTIN2* (*At3g18780*) and *UBQ10* (*At4g05320*) as housekeeping genes. Primer sequences used for gene expression analyses are listed in Table S1. qRT-PCR analyses were always performed on at least three biological replicates.

2.4 | Determination of polyamine levels

The levels of free Put, Spd and Spm were determined by high-performance liquid chromatography (HPLC) separation of dansyl derivatives, as described in (Zhang et al., 2023). Analyses were performed in four biological replicates per point of analysis.

2.5 | RNA-seq gene expression analyses

Pst DC3000 (OD_{600} = 0.001) and mock (10 mM $MgCl_2$) inoculation treatments were performed in three biological replicates using three different plants per genotype and treatment. Infiltration was performed as described above. Only infiltrated leaves were collected at 24 h of treatment for total RNA extraction. Total RNA was extracted using *TriZol* (Thermo Fisher) and further purified using RNeasy kit (Qiagen) according to manufacturer's instructions. Total RNA was quantified in Qubit fluorometer (Thermo Fisher) and checked for purity and integrity in a *Bioanalyzer-2100* device (Agilent Technologies). RNA samples were further processed at the Beijing Genomics Institute (BGI) for library preparation and RNA-seq using DNBSEQ. Libraries were prepared using the MGIEasy RNA Library Prep kit (MGI Tech) according to manufacturer's instructions and each library was paired-end sequenced (2 × 100 bp) on DNBSEQ-G400 sequencers. Read mapping and expression analyses were performed using the *CLC Genomics Workbench 21 version 21.0.5* (Qiagen). Only significant expression differences (fold-change ≥ 2; Bonferroni corrected $p \leq 0.05$) were considered. Gene Ontology (GO) analyses were performed using GO resource (http://geneontology.org) and PANTHER classification system (http://www.pantherdb.org/) with annotations from Araport11 (Carbon et al., 2019; Cheng et al., 2017; Mi et al., 2019). A binomial test was used to identify over-represented GO terms in the sample gene set compared with the reference genome set, using a significance threshold of $p < 0.05$ (Mi et al., 2013; Rivals et al., 2007).

2.6 | Proteomics analysis

Protein content of the samples in 7 M Urea buffer were determined using PIERCE™ 660 Protein Assay Kit (Thermo Scientific) following the product's specifications. Twenty micrograms of proteins from each sample were digested as follows: samples were reduced with 200 mM dithiothreitol (DTT) in 50 mM NH_4HCO_3 for 90 min at 32°C. The samples were then alkylated using 300 mM iodoacetamide in 50 mM NH_4HCO_3 and incubated in the dark for 30 min at room temperature. Another round of 200 mM DTT was added to do the quenching, and an appropriate amount of 50 mM NH_4HCO_3 was added to dilute the urea to a final concentration of 1 M. Digestion was done in two steps: an initial digestion with 1:20 (w/w) trypsin 0.1 μg μL^{-1} (sequence grade-modified trypsin, Promega) for 2 h at 32°C followed by a digestion with 1:20 (w/w) trypsin 0.1 μg μL^{-1} for 16 h at 32°C. Finally, the resulting peptide mixtures were acidified with formic acid (FA) and concentrated in a SpeedVac vacuum system (Eppendorf). Peptides were cleaned up with C18 tips (P200 top tip, PolyLC Inc.). Briefly, peptides were loaded on the tip columns (previously washed with 70% acetonitrile [ACN] in 0.1% FA and

equilibrated with 0.1% FA) by centrifugation at 350*g* for 2 min. Columns were washed twice with 100 µL 0.1% FA by centrifugation (350*g* for 2 min) and then peptides eluted in 2 × 80 µL of 50% ACN and 0.1% FA by centrifugation (350*g* for 2 min and 900*g* for 1 min). The peptides were dried-down in Speed Vacuum (Eppendorf) and delivered to IRB (Institute for Research in Biomedicine) Mass Spectrometry and Proteomics Core Facility to perform LC–tandem mass spectrometry (MS/MS) analysis. Raw data obtained in the MS analyses were processed with MaxQuant software (v_1.6.6.0). The spectra were searched using its built-in Andromeda search engine, against the SwissProt *Arabidopsis thaliana* database (v_220419) including contaminants. The following parameters were used: fixed modifications: carbamidomethylation of cysteins (C); variable modifications: methionine (M) oxidation and deamidation of asparagine and glutamine (NQ); enzyme: trypsin; maximum allowed missed cleavage: 2; match between runs and alignment time window were set to 0.7 and 20 min, respectively. Other nonspecified parameters were left as default. For label-free quantification, minimum ratio count was set to 1 and both razor and unique peptides were used for quantification. False discovery rate was set to 1% for both protein and peptide spectrum match levels. Label-free quantitative data were processed using Perseus open software (v. 1.6.15.0). Perseus was used to obtain the curated protein data set, which was built by removing from the list of identified proteins, those proteins identified as contaminants, proteins identified only by site, and proteins identified from the redundant and reversed databases. In addition, data were base 2 log transformed, and missing values were excluded unless three valid values were present in at least one group. Finally, imputation was done using normal distribution method. To test for differentially accumulated proteins, Student's *T* test was applied to the curated proteins and absolute fold-change values calculated.

2.7 | *Pst* DC3000 disease resistance assays

P. syringae pv. *tomato* DC3000 (*Pst* DC3000) was inoculated in 5-week-old plants by spray inoculation using a bacterial suspension (OD_{600} = 0.1) in 10 mM $MgCl_2$ and 0.04% Silwet L-77. *Pst* DC3000 colony forming units cm^{-2} were determined at 24, 48 and 72 h postinoculation as described (Liu et al., 2020a; Zhang et al., 2023).

2.8 | *B. cinerea* disease resistance assays

Spores of *B. cinerea* (CECT2100 obtained from the Spanish Collection of Type Cultures at Universidad de Valencia) cultivated in Potato Dextrose Agar medium were collected, washed with sterile water, counted and diluted to 4×10^6 spores mL^{-1} in inoculation buffer (Gamborg's B5 medium [Duchefa Biochemie] with 2% sucrose). The spores were incubated 2 h at room temperature and gentle agitation before inoculation on 5-week-old plant leaves, by placing 10 µL droplets of the spore suspension. Inoculated plants were covered with a transparent plastic dome to maintain high humidity and returned to the growth chamber. Leaves were photographed at 72 h postinoculation. Images were used to determine the lesion area using ImageJ (https://imagej.nih.gov).

Quantitative PCR (qPCR)-based quantification of fungal growth was determined by quantification of fungal and plant DNA (Gachon & Saindrenan, 2004). Five-week-old plants were spray-inoculated with a suspension of 5×10^5 spores mL^{-1} in inoculation buffer (Gamborg's B5 medium [Duchefa Biochemie] with 2% sucrose). Leaf samples were taken at 24 and 48 h of inoculation and the fungal and plant DNA was extracted using DNeasy Plant Minikit (Qiagen) according to manufacturer's instructions (Gachon & Saindrenan, 2004). The analysis was performed in six independent biological replicates, each containing three leaves from three different plants. The *B. cinerea β-tubulin* and *Arabidopsis Actin2* genes were used for real-time PCR analyses using specific primers listed in Supporting Information: Table S1.

2.9 | Quantification of SA, JA, JA-Ile and OPDA

Phytohormone analysis was performed as described in (Šimura et al., 2018) with some modifications. Briefly, around 20 mg of dry material were extracted in 1 mL ACN:water 1:1 (v:v) solution using a ball mill equipment (MillMix 20, Domel) at 17 rps for 10 min, adding a mixture containing 25 ng of ^{13}C-SA and dihydrojasmonic acid, as internal standards. After this, samples were sonicated for 5 min (Elma S30, Elma) and centrifuged for 10 min at 4000*g* and 4°C. The supernatant was filtered through solid-phase extraction (SPE) columns (Oasis HLV 30 mg 1 cc, Waters), taking the obtained eluent in new tubes and adding 0.5 mL 30% ACN to the SPE columns, which was also recovered with the previous eluent. Finally, the obtained samples were injected in an ultra-performance LC-MS (UPLC-MS) system (Xevo TQ-S, Waters). The chromatographic separation was achieved using a reverse phase C18 column (Luna Omega C18 50 × 2.1 mm, 1.8 µm particle size, Phenomenex) and a gradient of ultrapure deionized water and ACN, both supplemented with 0.1% FA at a flow rate of 0.3 mL min^{-1}. The phytohormones were detected with a triple quadrupole mass spectrometer coupled through a Z-spray electrospray ion source, configured in MRM mode. Finally, hormone levels were quantified in the samples through the interpolation of the obtained response in a standard curve, and the data was processed with the Masslynx v4.2 software.

2.10 | Stomatal assays

Leaf peels were obtained using clear adhesive tape from the abaxial side of mature leaves from 5-week-old wild-type plants. The leaf peels were immediately placed in contact with 20 mL of buffer solution (25 mM MES, 10 mM KCl, pH 6.15) or *Pst* DC3000 bacteria resuspended in buffer solution (OD_{600} = 0.001) (Zeng & He, 2010). The leaf peels were incubated in the different solutions for 1 and 4 h before being mounted on glass slides and directly observed under a light microscope. A minimum of 30 images from at least 10

independent leaf peels per treatment were randomly taken and stomata recorded for each sample treatment. Stomatal apertures were measured from images using ImageJ (https://imagej.nih.gov).

2.11 | Acyl CoA oxidase assays

Acyl-CoA oxidase activity assays were performed according to previously described methods (Adham et al., 2005; Gerhardt, 1987; Hryb & Hogg, 1979). Seeds of *spms* and wild-type plants were sterilized in 30% sodium hypochlorite supplemented with 0.5% Triton X-100 (Merck) for 10 min, followed by three washes with sterile distilled H_2O. Seeds were sown on growth media containing 1/2 MS salts supplemented with vitamins (Duchefa Biochemie), 0.5% sucrose, 0.6% plant agar (Duchefa Biochemie) and 0.05% MES adjusted to pH 5.7 with 1 M KOH. To synchronize germination, plates were stratified in the dark at 4°C during 2–3 days. Plates were incubated under 16 h light/8 h dark cycles at 20°C–22°C and 100–125 µmol photons m^{-2} s^{-1} of light intensity for 3 days. At 3 days after germination, around 100 mg of tissue was harvested per biological replicate, weighted and frozen immediately in liquid nitrogen. The tissue was ground to a powder using a mortar and pestle. The ground tissue was added 1 mL of cold extraction buffer (50 mM potassium phosphate buffer pH 7.6, 50 µM FAD, 100 µg mL^{-1} bovine serum albumin [BSA], 0.025% Triton X-100) supplemented with 10 µL of protease inhibitor cocktail (P9599, Merck). Extracts were centrifuged at 12 000*g* and 4°C for 15 min. For each replicate, 100 µL of enzyme supernatant was combined with 100 µL of reaction buffer (0.8 mM fatty acyl-CoA substrate, 50 mM potassium phosphate buffer pH 7.6, 50 µM FAD, 100 µg mL^{-1} BSA, 0.025% Triton X-100, 110 U horseradish peroxidase, 50 mM *p*-hydroxybenzoic acid and 2 mM 4-aminoantipyrine). Reactions were monitored spectrophotometrically at 500 nm to detect H_2O_2 production as an indirect measure of acyl-CoA oxidase activity. A H_2O_2 standard curve was used to determine H_2O_2 concentrations in the extracts and calculate reaction rates (mmol H_2O_2 g^{-1} min^{-1}). All chemicals were purchased from Merck.

2.12 | Root growth assays

Seeds of the different genotypes were sterilized in 30% sodium hypochlorite supplemented with 0.5% Triton X-100 (Merck) for 10 min, followed by three washes with sterile distilled H_2O. Seeds were sown, stratified, and germinated on 50 mL vertical plates containing 1/2 MS salts supplemented with vitamins (Duchefa Biochemie), 1% sucrose, 0.8% plant agar (Duchefa Biochemie) and 0.05% MES pH 5.7. The media was supplemented with methyl jasmonate (100 µM MeJA, Merck), COR (1 µM COR, Merck), tunicamycin (1 µg mL^{-1} TM, Merck), 2,4-dichlorophenoxybutyric acid (0.2 µg mL^{-1} 2,4-DB, Merck), 2,4-dichlorophenoxyacetic acid (0.05 µg mL^{-1} 2,4-D, Merck) or mock (0.1% dimethyl sulfoxide [DMSO] in water), as required. After 12 days of growth at 16 h light/8 h dark cycles, 20°C–22°C and 100–125 µmol photons m^{-2} s^{-1} of light intensity, pictures were taken and the primary root length of the seedlings measured using ImageJ (https://imagej.nih.gov).

2.13 | Untargeted lipidomics analyses

One hundred milligrams of leaves from 5-week-old *spms* and wild-type plants were used for an untargeted lipidomics analysis using five biological replicates. The analyses were performed at the BGI. The different samples were spiked with internal standards 15:0-18:1(d7)PC, 18:1-d7 Lyso PE, 15:0-18:1(d7)PS (Avanti Polar Lipids) and extracted in methyl tert-butyl ether/methanol (MeOH) (3:1 v/v) precooled at −20°C. Tissue lysis was performed in a tissue grinder device (50 Hz, 5 min), followed by bath ultrasonication for 15 min and precipitation at −20°C for 2 h. Afterwards, 0.5 mL of (H_2O/MeOH 3:1 v/v) was added to each sample and vortexed for 1 min. Samples were centrifuged at 24 000*g* for 10 min and 0.6 mL of the supernatant taken and dried. Before LC-MS analysis, the extracts were reconstituted in 400 µL isopropanol containing 10 mM ammonium acetate. For quality control, 50 µL of supernatant from each sample were mixed. The UPLC-MS analysis was performed on a Waters UPC I-Class Plus (Waters) tandom Q Exactive high resolution mass spectrometer (Thermo Fisher Scientific) for separation and detection of lipids. Chromatographic separation was performed on CSH C18 Column (1.7 µm 2.1 × 100 mm, Waters). At positive ion mode with mobile phase A consisting of 60% ACN in water + 10 mM ammonium formate + 0.1% FA and mobile phase B consisting of 90% isopropanol + 10% ACN + 10 mM ammonium formate + 0.1% FA. At negative ion mode, with mobile phase A consisting of 60% ACN in water + 10 mM ammonium formate and mobile phase B consisting 90% isopropanol + 10% ACN + 10 mM ammonium formate. The column temperature was maintained at 55°C. The gradient conditions were as follows: 40% ~ 43% B over 0 ~ 2 min, 43% ~ 50% B over 2 ~ 2.1 min, 50% ~ 54% B over 2.1 ~ 7 min, 54% ~70% B over 7 ~ 7.1 min, 70% ~ 99% B over 7.1 ~ 13 min, 99% ~ 40% B over 13 ~ 13.1 min, held constant at 99% ~ 40% B over 13.1 ~ 15 min and washed with 40% B over 13.1–15 min. The flow rate was 0.4 mL min^{-1} and the injection volume was 5 µL. Q Exactive (Thermo Fisher Scientific) was used for primary and secondary MS data acquisition. The full scan range was 70–1050 *m/z* with a resolution of 70 000 and the automatic gain control (AGC) target for MS acquisitions was set to 3e6 with a maximum ion injection time of 100 ms. Top three precursors were selected for subsequent MSMS fragmentation with a maximum ion injection time of 50 ms and resolution of 17 500, the AGC was 1e5. The stepped normalized collision energy was set to 15, 30 and 45 eV. Electrospray ionization parameters were setting as follows: Sheath gas flow rate was 40, Aux gas flow rate was 10, positive-ion mode Spray voltage (|KV|) was 3.80, negative-ion mode Spray voltage (|KV|) was 3.20, Capillary temperature was 320°C, and Aux gas heater temperature was 350°C. Lipid identification was performed on Lipidsearch v.4.1 (Thermo Fisher Scientific). Data preprocessing included (i) removing metabolites with >50% missing values in QC samples and more than 80% missing values in experimental samples. (ii) Filling in missing values

with k-nearest neighbour algorithm. (iii) Normalizing the data to obtain relative peak areas by probabilistic quotient normalization (Di Guida et al., 2016). (iv) Using quality control-based robust locally estimated scatterplot smoothing signal correction to correct Batch effect (Dunn et al., 2011). (v) Removing metabolites with a coefficient of variation >30% on their Relative peak area in QC samples. Values for each identified lipid were expressed as relative content (mol%).

2.14 | ER stress, COR and ABA treatments

Wild-type and *spms* seedlings were grown in half-strength MS medium and 1% sucrose under 16 h light/8 h dark cycles at 20°C–22°C and 100–125 µmol photons m^{-2} s^{-1} of light intensity for 10 days. The seedlings were transferred to liquid MS medium supplemented with 1 µg mL^{-1} TM, 100 µM Brefeldin A (BFA), 100 µM DTT or mock (0.1% DMSO) for 6–24 h. Samples were collected for qRT-PCR gene expression analyses and/or polyamine levels determination. For COR and ABA treatments, 10-day-old seedlings grown on half-strength MS medium were transferred to the same media containing 1 µM COR or 5 µM ABA. Samples were harvested at 24 h of treatment for qRT-PCR gene expression analyses.

3 | RESULTS

3.1 | Polyamine responses to *Pst* DC3000 and their dependence on COR, SA and JA signalling

To study the modulation of polyamine metabolism and the role of Spm during the defence response to *Pst* DC3000, we first determined the changes in expression of all polyamine biosynthesis and oxidation genes in both wild-type and *spms* plants at 24 and 48 h of bacterial and mock inoculation (Figure 1b). Inoculation with *Pst* DC3000 consistently increased the expression of *ARGININE DECARBOXYLASE 2* (*ADC2*), *SPERMINE SYNTHASE* (*SPMS*), *S-ADENOSYLMETHIONINE DECARBOXYLASE 3* (*SAMDC3*), and *COPPER-CONTAINING AMINE OXIDASE δ2* (*CuAOδ2*). The expression levels in the wild-type and *spms* mutant were comparable for all genes, except for *SPMS*, which expression was undetectable in the mutant (Figure 1b). Interestingly, inoculation with the COR-deficient strain *Pst* DC3000 Δ*cor* (Ma et al., 1991) compromised the transcriptional activation of *ADC2* at both 24 and 48 h, and that of *SPMS*, *SAMDC3* and *CuAOδ2* at 24 h (Figure 2a). Consistent with the *ADC2* expression, *Pst* DC3000 Δ*cor* inoculation also led to lower increases in Put compared with *Pst* DC3000 treatment (Figure 2b). The data indicated that COR triggers

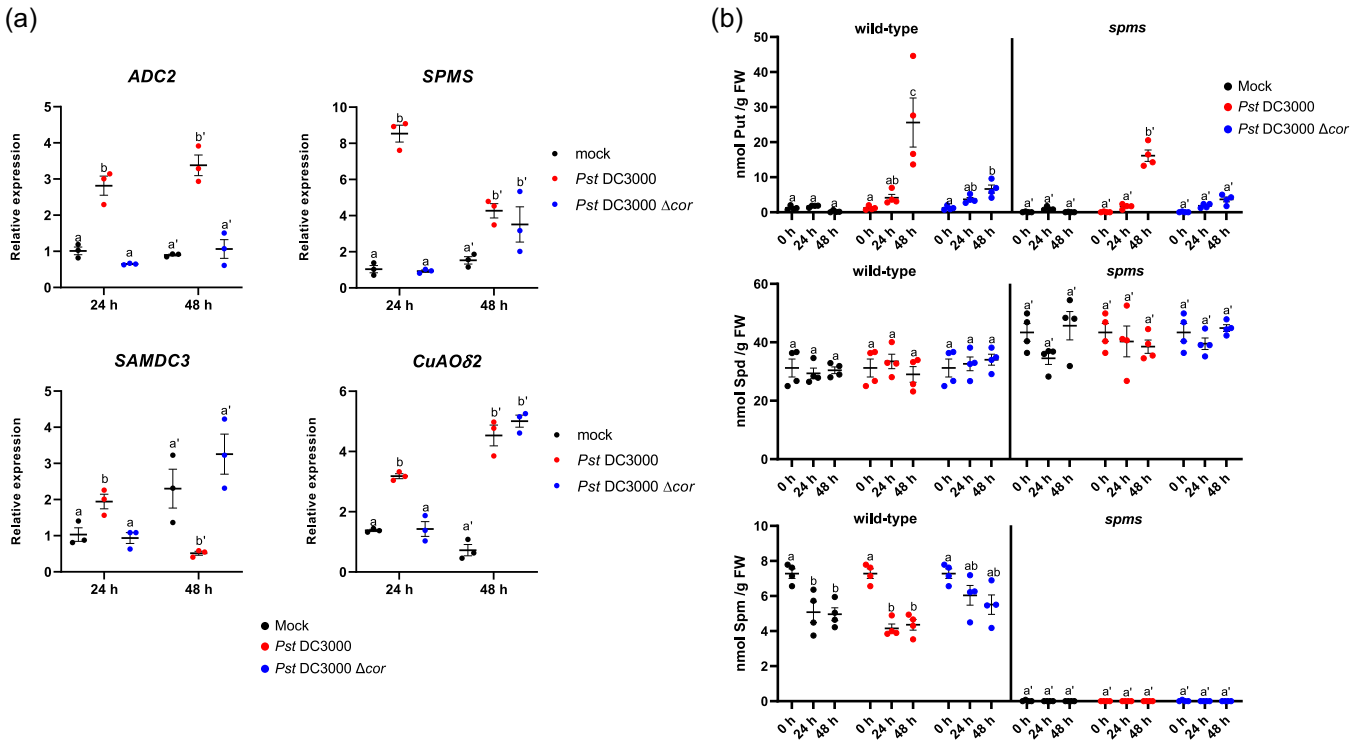

FIGURE 2 Effect of coronatine (COR) on the elicitation of polyamine metabolism. (a) Expression analyses of polyamine biosynthesis genes *ADC2* (*ARGININE DECARBOXYLASE 2*), *SPMS* (*SPERMINE SYNTHASE*), *SAMDC3* (*S-ADENOSYLMETHIONINE DECARBOXYLASE 3*) and polyamine oxidation CuAOδ2 (*COPPER AMINE OXIDASE δ2*) in response to *Pst* DC3000 (OD_{600} = 0.001), COR-deficient *Pst* DC3000 Δ*cor* (OD_{600} = 0.001) and mock (10 mM $MgCl_2$) infiltration, determined in wild-type plants at 24 and 48 h of treatment. Expression values are relative to the wild-type (mock) treatment and represent the mean ± SD from three biological replicates per point of analysis. (b) Concentrations of putrescine (Put), spermidine (Spd) and spermine (Spm) at 0, 24, and 48 h of *Pst* DC3000, *Pst* DC3000 Δ*cor* and mock (10 mM $MgCl_2$) inoculation. Values represent the mean ± SD from four biological replicates per point of analysis. Different letters indicate significant differences ($p < 0.05$) according to two-way analysis of variance followed by Tukey's posthoc test. [Color figure can be viewed at wileyonlinelibrary.com]

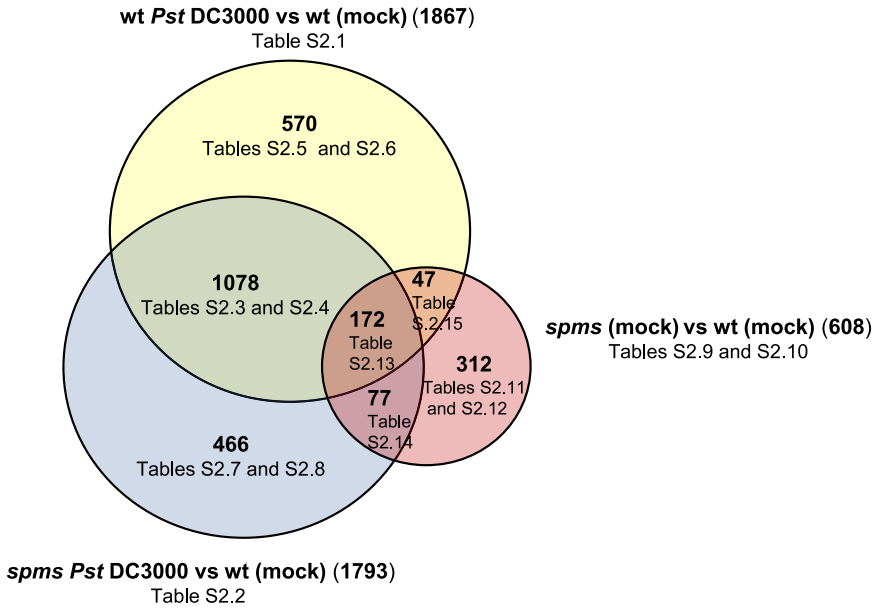

FIGURE 3 RNA sequencing analyses of *spms* and wild-type (wt) plants infiltrated with *Pst* DC3000 (OD_{600} = 0.001) or mock (10 mM $MgCl_2$). Venn diagram of differentially expressed genes (fold change ≥ 2; Bonferroni corrected *p*-value < 0.05) in *spms* and wt plants at 24 h of treatment. A detailed list of genes and Gene Ontology terms is found in Supporting Information: Tables S2.1–S2.18. [Color figure can be viewed at wileyonlinelibrary.com]

important changes in polyamine metabolism during the defence response to *Pst* DC3000, thus pointing to polyamine metabolism as potential target to modify defence responses.

To investigate the involvement of JA and SA pathways in the regulation of polyamine metabolism, we performed a detailed analysis of *ADC2*, *SPMS*, *SAMDC3*, and *CuAOδ2* expression (Supporting Information: Figure S1) and measured polyamine levels (Supporting Information: Figure S2) in response to *Pst* DC3000 in *coi1-1*, *myc2*, *sid2-1*, *eds1-2*, *npr1-1* and wild-type plants. The *coi1-1* and *myc2* mutants showed compromised upregulation of *ADC2*, *SPMS* and *SAMDC3* expression in response to *Pst* DC3000, providing evidence for the involvement of the JA pathway in the regulation of polyamine metabolism. Conversely, *CuAOδ2* expression was not consistently affected by *coi1-1* or *myc2* mutations. The upregulation of *SPMS* and *SAMDC3* expression was also dampened by the *sid2-1*, *eds1-2* and *npr1-1* mutations, whereas higher *ADC2* expression was observed in *npr1-1* at 48 h of *Pst* DC3000 inoculation (Supporting Information: Figure S1). After 48 h of *Pst* DC3000 treatment, Put accumulation in *coi1-1* and *myc2* mutants was significantly lower than in the wild type, in correlation with *ADC2* expression. In contrast, Put levels in *sid2-1*, *eds1-2*, *npr1-1* and *spms* mutants were almost twofold higher than the wild-type (Supporting Information: Figure S2). Remarkably, *adc2* but not *adc1* mutants exhibited compromised accumulation of Put in response to *Pst* DC3000 inoculation, providing evidence that ADC2 is the major contributor to Put biosynthesis in response to *Pst* DC3000 and that the polyamine originates from the plant rather than the bacteria (Supporting Information: Figure S3).

Collectively, these results indicated that functional COI1 and MYC2 are required for *ADC2* responsiveness to *Pst* DC3000 and Put accumulation, this being a SA-independent response. On the other hand, both COI1/MYC2 and EDS1/SA/NPR1 signalling modules are required for the full activation of *SPMS* and *SAMDC3* expression in response to *Pst* DC3000. *CuAOδ2* responses were attenuated in *sid2-1*, *eds1-2* and *npr1-1* mutants. The high Put levels found in the susceptible genotypes *sid2-1*, *eds1-2*, *npr1-1* and *spms* inoculated with *Pst* DC3000, suggested a correlation between Put levels and the progression of bacteria growth. Alternatively, it may result from the potentiation of JA responses in SA pathway (Spoel et al., 2003) or *spms* mutants (this work). Taken together, these findings indicated that both JA and SA play crucial roles in modulating polyamine metabolism in response to *Pst* DC3000, with a major contribution of COR and JA-signalling to the modulation of Put levels.

3.2 | RNA-seq expression analyses shed light on the role of Spm in modulating SA, JA and ER stress in response to *Pst* DC3000

To investigate in deeper detail the contribution of Spm to the defence response to Pst DC3000, we performed RNA-seq gene expression analyses in *spms* and wild-type plants at 24 h of *Pst* DC3000 and mock inoculation (Figure 3 and Supporting Information: S4A and Tables S2.1–S2.18). Significant alterations in gene expression were observed following *Pst* DC3000 treatment, with 1867 and 1793 genes being differentially expressed in the wild type and *spms*, respectively (fold change ≥ 2; Bonferroni corrected *p*-value < 0.05; Supporting Information: Tables S2.1 and S2.2). Treatment with *Pst* DC3000 resulted in the differential expression of 1078 common genes in both genotypes (Supporting Information: Table S2.3), which represented 58% and 60% of the total genes exhibiting significant expression changes in the wild type and *spms*, respectively (Figure 3). As expected, upregulated genes within the common expression sector were related to defence responses to bacterium, SA responses, SAR, ROS signalling, oxidative stress, as well as other GO terms (Supporting Information: Table S2.4). Despite

the overlap, noticeable differences in gene expression were observed between the genotypes in important genes related to SA metabolism and SAR establishment: *ICS1*, *EDS5*, *PBS3*, *SARD1*, *FMO1*, and *ALD1*; and ER stress signalling *BINDING PROTEIN 3* (*BIP3*), *PROTEIN DISULFIDE ISOMERASE-LIKE 1-1* (*PDIL1-1*) and *PDIL1-2* (Figure 4a and Supporting Information: Table S2.3).

Pst DC3000 treatment also elicited the differential expression of 570 genes specifically in wild-type plants ('wild-type *Pst* DC3000 only'; Supporting Information: Table S2.5). The expression of genes within this sector showed moderate correlation between wild-type and *spms* mutant ($r^2 = 0.77$) (Supporting Information: Figure S4B), which suggested a genotype-specific response. The 'wild-type *Pst* DC3000 only' sector was enriched in genes related to JA responses, lipid metabolism and wounding (Figure 3 and Supporting Information: Tables S2.5 and S2.6). The data suggested that JA transcriptional activation was compromised in *spms* at 24 h of *Pst* DC3000 treatment. Other 466 genes were deregulated only in the *spms* mutant in response to *Pst* DC3000 ('*spms Pst* DC3000 only'; Figure 3 and Supporting Information: Table S2.7). The expression of genes in this sector was also moderately correlated ($r^2 = 0.70$) between the genotypes (Supporting Information: Figure S4B). The '*spms Pst* DC3000 only' sector was enriched in genes associated with ER stress signalling (Supporting Information: Table S2.8).

Under basal conditions, without any type of treatment, the *spms* mutant already showed 91 differentially expressed genes, of which only five were upregulated compared with the wild type. Among these, the most upregulated gene in *spms* was *DELTA 9 ACYL-LIPID DESATURASE 1* (*ADS1*), which is involved in fatty acid desaturation (Supporting Information: Table S3.1 and Figure S5). This further suggested a potential impact of Spm deficiency on lipid metabolism. Downregulated genes in *spms* were enriched in GO terms related to defence and SA responses (Supporting Information: Tables S3.1–S3.3). They included key genes in SA biosynthesis and signalling: *SARD1*, *CBP60g*, *PBS3*, *WRKY46* and *PATHOGENESIS-RELATED GENE 1* (*PR1*) (Supporting Information: Figure S5). The data further suggested a role for Spm in regulating SA responses. Overall, RNA-seq analyses indicated that the deficiency of Spm leads to altered transcriptional activation of both JA and SA pathways, as well as expression changes compatible with ER stress in response to *Pst* DC3000.

3.3 | Spm deficiency compromises SA-mediated defence responses to *Pst* DC3000

We further investigated the impact of Spm deficiency on SA-mediated immune signalling in response to *Pst* DC3000 by examining the expression of SA metabolism and signalling genes by qRT-PCR in both *spms* and wild type plants at 24 and 48 h postbacterial and mock inoculation (Figure 4b). Consistent with the RNA-seq data, the expression levels of important SA biosynthesis and signalling genes (*ICS1*, *EDS5*, *PBS3*, *PAD4*, *CBP60g*, *SARD1*), and SA-inducible *PR1* were significantly lower in *spms* relative to the wild type at 24 h of *Pst* DC3000 inoculation (Figure 4b). In addition, *spms* exhibited delayed transcriptional activation of SAR-related genes *ALD1* and *FMO1* (Figure 4b). In agreement with the expression data, *spms* accumulated lower SA than the wild-type under basal conditions (0 h) and at 48 h of *Pst* DC3000 treatment (Figure 4c). The results indicated that Spm deficiency dampened SA-mediated immune responses to *Pst* DC3000. The decrease in SA responses correlated with a significant increase in *Pst* DC3000 growth in *spms* compared with the wild type at 72 h of *Pst* DC3000 spray inoculation (Figure 4d).

3.4 | Spm deficiency elicits JA biosynthesis and signalling

To further analyse the contribution of Spm to the transcriptional activation of the JA pathway in response to *Pst* DC3000, we performed qRT-PCR gene expression analyses of JA metabolism genes in both the wild type and *spms* at 24 and 48 h of *Pst* DC3000 and mock inoculation (Figure 5). Compared with the wild type, the *spms* mutant showed delayed transcriptional activation, but eventually equal or stronger expression of JA biosynthesis genes *LOX2*, *LOX3*, *AOC1*, *OPR3*, *OPC-8:0 COA LIGASE1* (*OPLC1*) and jasmonoyl-isoleucine-12-hydroxylase *CYTOCHROME P450 FAMILY 94 SUB-FAMILY B POLYPEPTIDE 3* (*CYP94B3*) in response to *Pst* DC3000. A similar response was observed for JA signalling genes *MYC2*, *JAZ1*, *JAZ9* and *JAZ10* (Figure 6). At 48 h after *Pst* DC3000 inoculation, *spms* also exhibited significantly higher expression of JA-marker genes *VEGETATIVE STORAGE PROTEIN 1* and *2* (*VSP1* and *VSP2*), which are related to the MYC2-branch of JA signalling (Lorenzo et al., 2004) (Figure 6). The data suggested the occurrence of a delayed but stronger transcriptional activation of the JA-MYC2 pathway in *spms*. To further study the effect of Spm deficiency on JA biosynthesis, we determined the concentrations of JA, JA-Ile and OPDA in *spms* and wild-type plants at 0, 24, and 48 h of *Pst* DC3000 and mock inoculation. As shown in Figure 7, JA and JA-Ile levels were higher in *spms* than in the wild type already under basal conditions (0 h) and in response to the different treatments. The levels of the JA precursor, OPDA, were also higher in *spms* than in the wild type upon *Pst* DC3000 inoculation. The data indicated that JA biosynthesis was stimulated in *spms*. In agreement with this, the *spms* mutant exhibited higher sensitivity to MeJA and COR treatments in root growth inhibition assays (Supporting Information: Figure S6).

3.5 | Analysis of the *spms* proteome

Owing to the elevated levels of JA in *spms* under basal conditions, we conducted a proteomics analysis to identify proteins that accumulated differentially between *spms* and wild type plants in the absence of pathogen infection. Of the 1612 proteins quantified in both genotypes, 59 showed 1.3-fold or higher differences in abundance between *spms* and the wild type (Supporting Information: Figure S7A and Table S4.1). Among proteins significantly more abundant in *spms* than in the wild type, we found an enrichment in biological processes

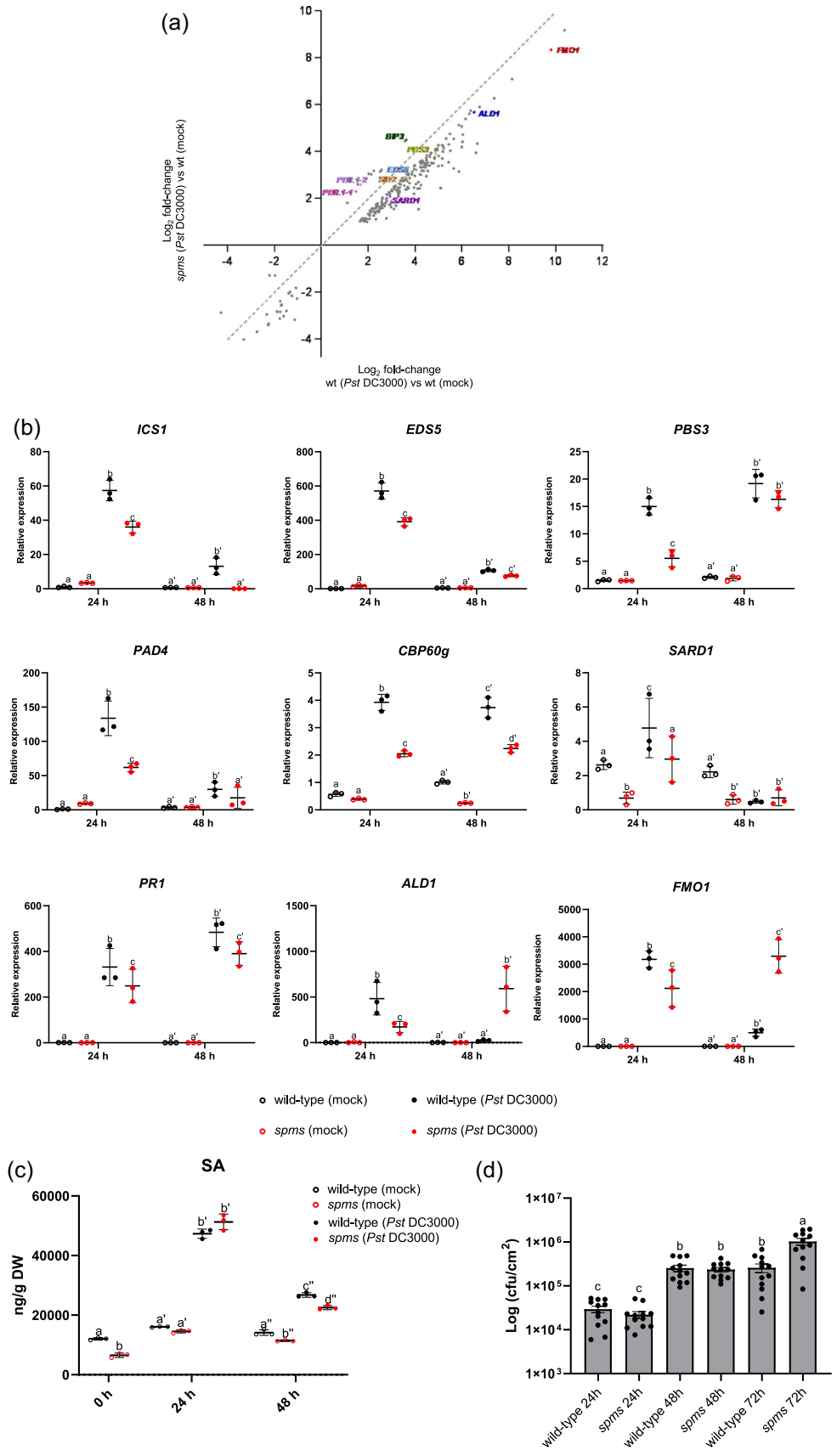

FIGURE 4 (See caption on next page).

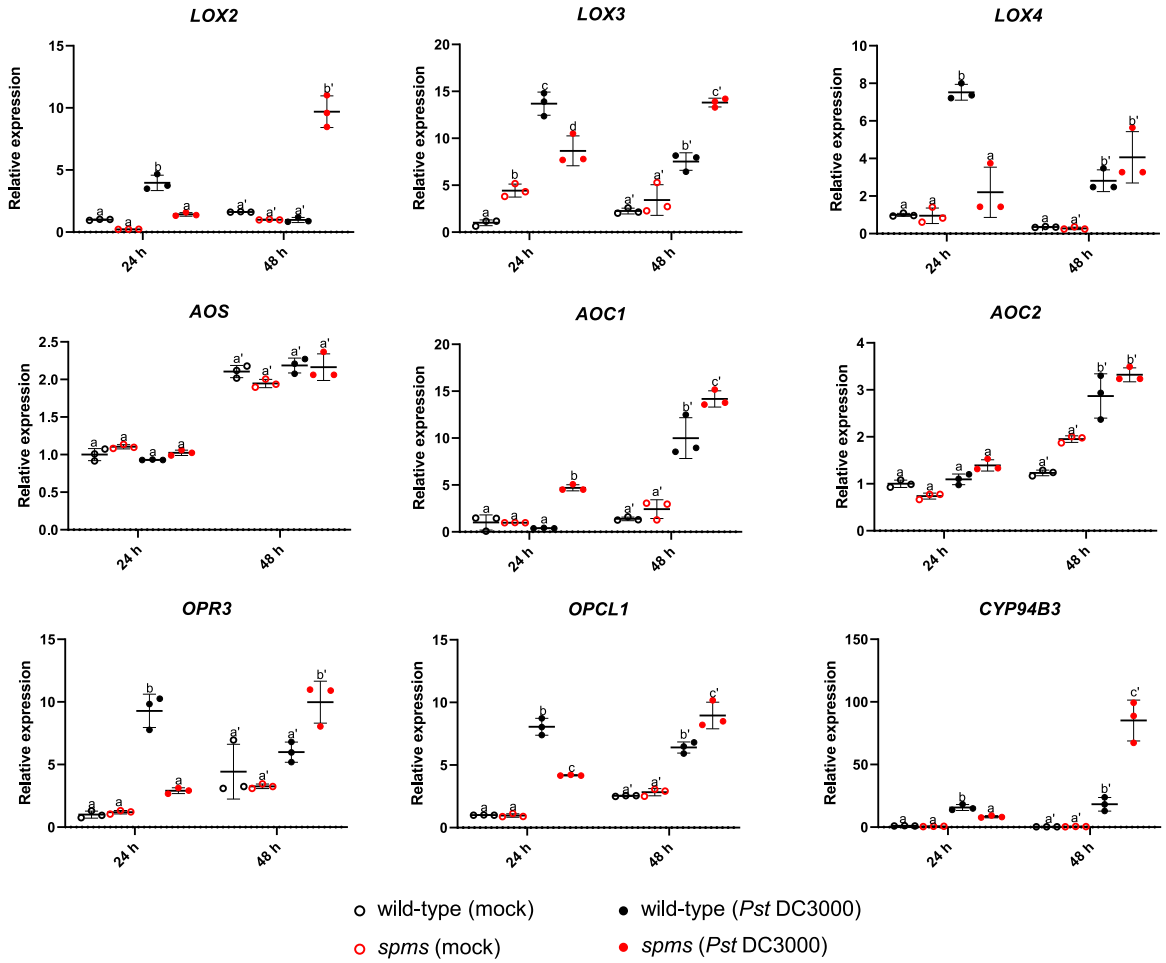

FIGURE 5 Expression analyses of jasmonic acid biosynthesis genes in wild type and *spermine synthase* (*spms*) plants at 24 and 48 h of *Pst* DC3000 (OD_{600} = 0.001) and mock (10 mM $MgCl_2$) infiltration. Values represent the mean ± SD from three biological replicates per point of analysis. Different letters indicate significant differences ($p < 0.05$) according to two-way analysis of variance followed by Tukey's posthoc test. AOC, allene oxide cyclase; AOS, allene oxide synthase; CYP94B3, jasmonoyl-isoleucine-12-hydroxylase; LOX, Lipoxygenase; OPCL1, OPC-8:CoA ligase 1; OPR3, OPDA reductase 3. [Color figure can be viewed at wileyonlinelibrary.com]

related to serine and oxoacid metabolism (Supporting Information: Table S4.2). Spm deficiency also led to increased abundance of JA-inducible KAT5 (3-KETO-ACYL-COENZYME A THIOLASE 5) (fold-change *spms*/wt = 1.39; $p = 0.010$) that encodes one of the three KAT enzymes catalysing the last step of β-oxidation (Castillo et al., 2004; Goepfert & Poirier, 2007; Wasternack & Feussner, 2018) and of the ER stress sensor protein FK506- AND RAPAMYCIN-BINDING PROTEIN 15 KD-2 (FKBP15-2) (Fan et al., 2018) (fold-change *spms*/wt = 5.13; $p = 0.03$). Lesser but still statistically significant differences in protein abundance were detected in AOC2 (fold-change *spms*/wt = 1.2; $p = 0.0016$) and the ER stress marker PDIL1-1 (fold-change *spms*/wt = 1.2; $p = 0.006$) (Supporting Information: Table S4.1). In contrast, *spms* accumulated lower levels of proteins associated with photosynthesis and water transport relative to the wild type (Supporting Information: Table S4.2). No correlation was detected between protein abundance and gene expression under

FIGURE 4 Effect of spermine (Spm) deficiency on salicylic acid (SA) metabolism. (a) Expression correlation of commonly deregulated genes in wild-type and *spermine synthase* (*spms*) mutant in response to *Pst* DC3000. Genes related to SA-mediated defences and endoplasmic reticulum (ER) stress are indicated. (b) Quantitative reverse-transcription polymerase chain reaction (qRT-PCR) gene expression analyses of SA metabolism and signalling, and systemic acquired resistance (SAR) establishment in wild-type and *spms* in response to *Pst* DC3000 (OD_{600} = 0.001) and mock (10 mM $MgCl_2$) infiltration, at 24 and 48 h of treatment. Expression values are relative to wild-type (mock) treatment and represent the mean ± SD from three biological replicates per point of analysis. (c) Quantification of SA levels in wild-type and *spms* in response to *Pst* DC3000 (OD_{600} = 0.001) and mock (10 mM $MgCl_2$) infiltration at 0, 24 and 48 h of treatment. (d) Disease resistance phenotypes to *Pst* DC3000 in wild-type and *spms* mutant at 24, 48 and 72 h of spray inoculation (OD_{600} = 0.1). Different letters indicate significant differences ($p < 0.05$) according to two-way analysis of variance followed by Tukey's posthoc test. [Color figure can be viewed at wileyonlinelibrary.com]

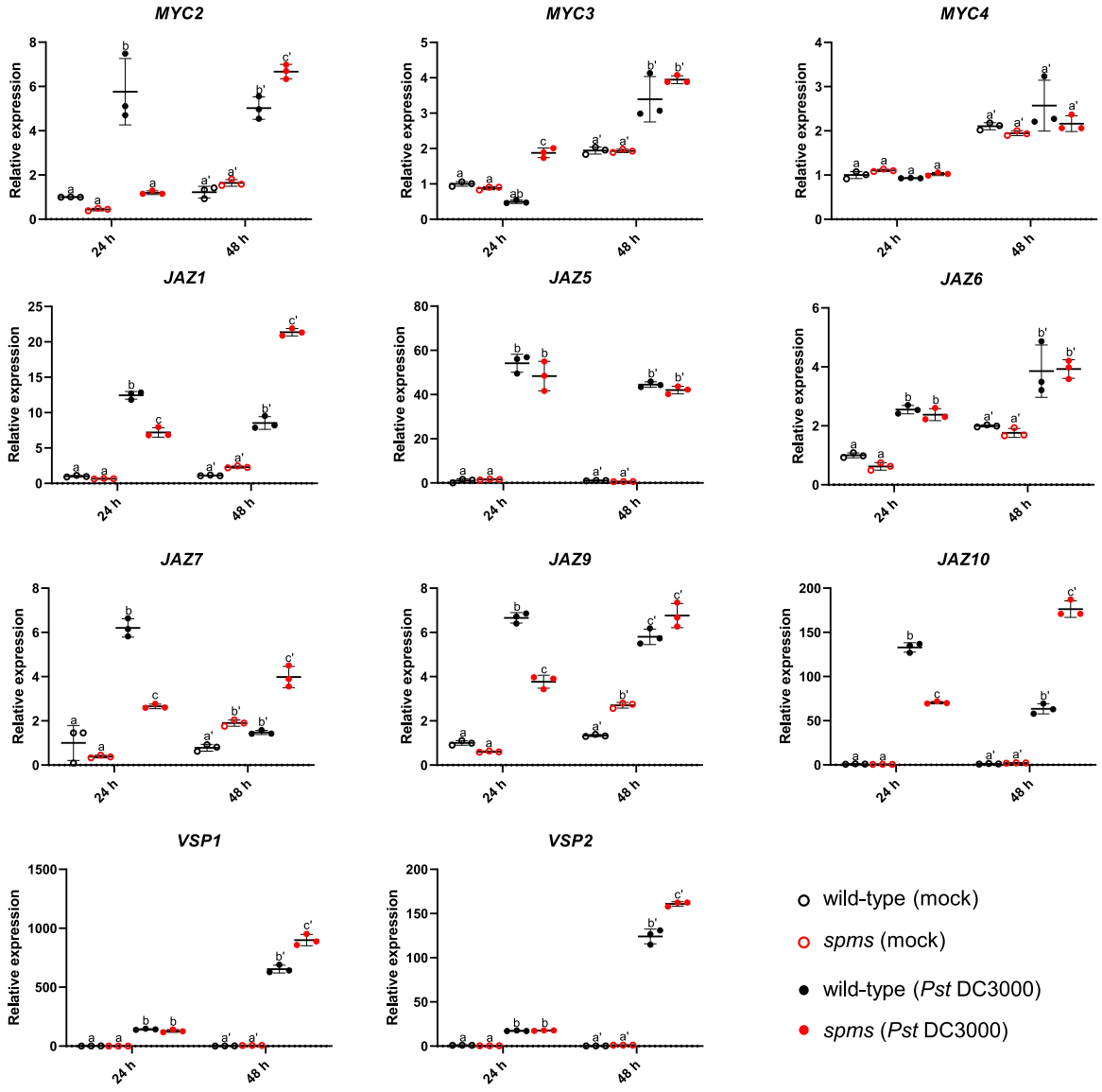

FIGURE 6 Expression analyses of jasmonic acid signalling genes in wild type and *spermine synthase* (*spms*) plants at 24 and 48 h of *Pst* DC3000 (OD_{600} = 0.001) and mock (10 mM $MgCl_2$) infiltration. Values represent the mean ± SD from three biological replicates per point of analysis. Different letters indicate significant differences ($p < 0.05$) according to two-way analysis of variance followed by Tukey's posthoc test. [Color figure can be viewed at wileyonlinelibrary.com]

basal conditions, which suggested a potential effect of polyamines on posttranscriptional regulation, translational control and/or protein degradation (Supporting Information: Figure S7B). Overall, the proteomics data pointed to the implication of Spm in the regulation of JA biosynthesis, ER stress signalling, amino acid and oxoacid metabolism, photosynthesis and water transport.

3.6 | JA-SA crosstalk in *spms*

We hypothesized that the constitutively high levels of JA in *spms* could reduce SA responses through crosstalk modulation. The bacterial phytotoxin COR mimics JA-Ile and activates the JA signalling pathway to boost bacterial virulence by suppressing SA-defences mediated by *ANAC019*, *ANAC055*, and *ANAC072*, thus providing a mechanism by which JA counteracts SA responses (Zheng et al., 2012). The expression of *ANAC019*, *ANAC055* and *ANAC072* is upregulated in response to COR, abscisic acid (ABA) and *P. syringae* treatments (Zheng et al., 2012). We then analysed *ANAC019*, *ANAC055* and *ANAC072* responsiveness in *spms* and wild-type plants challenged with these elicitors (Figure 8a). The expression of *ANAC019* was significantly higher in *spms* than in the wild-type under basal conditions and in response to COR, but not ABA. Conversely, no differences in *ANAC055* or *ANAC072* expression were detected in response to COR or ABA. In agreement with *ANAC019* expression, transcripts of the target genes *ICS1* and *BSMT1* exhibited significant differences between the genotypes in response to COR, but not in response to ABA (Figure 8a). *ICS1* expression in *spms* was lower than in the wild type under basal conditions and after COR treatment.

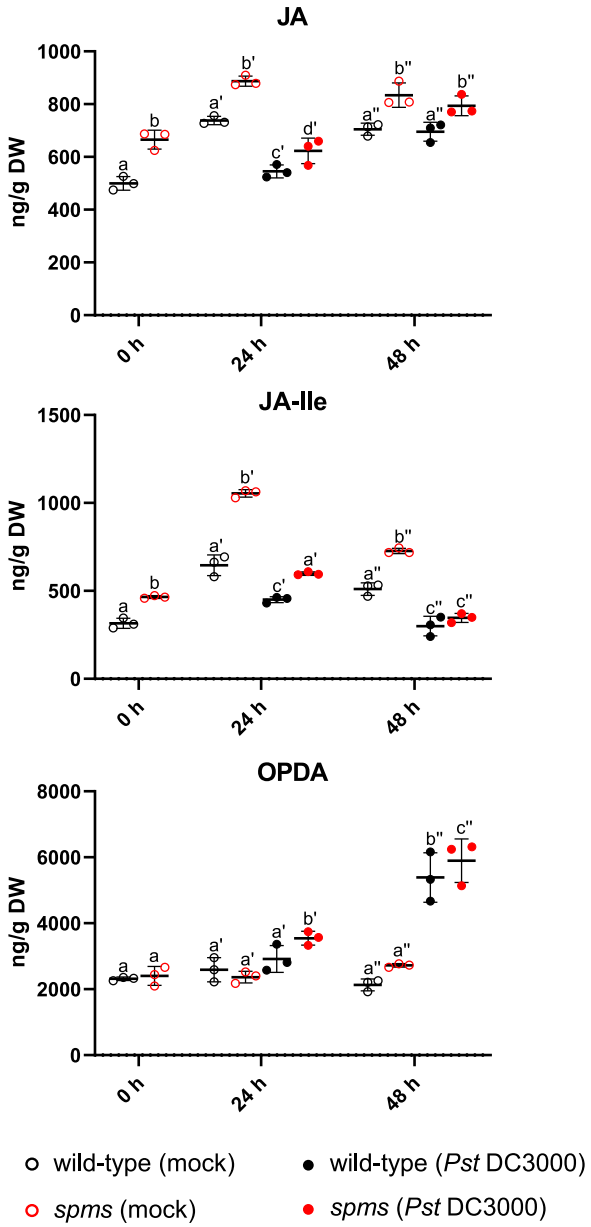

FIGURE 7 Quantification of jasmonic acid (JA), JA-isoleucine (JA-Ile) and 12-oxophytodienoic acid (OPDA) in wild-type and *spermine synthase* (*spms*) plants under basal conditions (0 h) and at 24 and 48 h of *Pst* DC3000 (OD_{600} = 0.001) and mock (10 mM $MgCl_2$) infiltration. Values represent the mean ± SD from three biological replicates per point of analysis. Different letters indicate significant differences ($p < 0.05$) according to two-way analysis of variance followed by Tukey's posthoc test.

In contrast, the expression of *BSMT1* resulted significantly higher in *spms* than in wild type plants after COR treatment. The increased expression of *VSP2* in *spms*, following COR treatment, provided further evidence for the stimulation of the JA pathway in the *spms* mutant. No significant differences in *SAGT1* expression were detected between the genotypes in response to COR or ABA (Figure 8a).

We further analysed the expression of *BSMT1*, *SAGT1* and *ANAC019* in response to *Pst* DC3000 and mock in both wild type and *spms* mutant plants, at 24 and 48 h of treatment (Figure 8b). These expression analyses revealed a substantial elevation of *ANAC019* and *BSMT1* transcripts in *spms*, as compared with wild type plants, upon exposure to *Pst* DC3000. Our findings indicated that lack of Spm causes a more pronounced deregulation of *ICS1* and *BSMT1* in correlation with *ANAC019* expression, in response to COR and *Pst* DC3000, resulting in decreased SA accumulation (Figures 4 and 8a,b).

3.7 | Stomata responses to *Pst* DC3000 are not affected by Spm deficiency

ANAC019, *ANAC055* and *ANAC072* are required for COR-triggered reopening of closed stomata to facilitate bacterial entry (Melotto et al., 2006). Based on the stronger JA and COR responses, as well as the differential modulation of *ANAC019* expression, we investigated whether Spm deficiency affected stomata responses to *Pst* DC3000 (Figure 8c). Stomata aperture was measured in *spms* and wild type leaf peels following 1 and 4 h incubation with *Pst* DC3000 and mock. The application of *Pst* DC3000 induced stomata closure at 1 h and reopening at 4 h in both *spms* and wild type leaf peels, with no significant variation between the two genotypes (Figure 8c). The results indicated that Spm deficiency does not affect stomata responses to bacteria.

3.8 | Effect of Spm deficiency on Acyl-CoA oxidase activity

In animal cells, Spd has been documented to stimulate mitochondrial β-oxidation of long-chain fatty acids by allosteric binding to hydroxyacyl-CoA dehydrogenase subunits α and β, which constitute the mitochondrial trifunctional protein complex. Interestingly, this Spd-mediated effect was found to be competitively inhibited by Spm (Al-Habsi et al., 2022). In plants, β-oxidation is involved in the latter steps of JA biosynthesis. Owing to the high levels of JA found in the *spms* mutant already under basal conditions, we determined whether Spm deficiency could lead to increased peroxisomal β-oxidation. To this aim, we determined acyl-CoA oxidase enzyme activities using different chain length fatty acyl-CoA substrates in extracts from 3-day-old light-grown *spms* and wild type seedlings. Our findings indicated that the acyl-CoA oxidase activity using *n*-hexanoyl-CoA (C6:0), lauroyl-CoA (C12:0) and stearoyl-CoA (C18:0) as substrates was similar between *spms* and wild type (Figure 9). Consistent with this, we found no differences on root growth phenotypes between *spms* and wild type seedlings grown in the presence of 2,4-DB or 2,4-D, which are used to identify genotypes affected in peroxisomal β-oxidation (Supporting Information: Figure S8) (Hayashi et al., 1998). The data indicated that the stimulation of JA biosynthesis in Spm-deficient plants was not due to increased β-oxidation. Rather, it correlated with higher MGDG levels and increased expression of genes involved in early steps of the JA biosynthesis pathway occurring in the chloroplast (Figure 5).

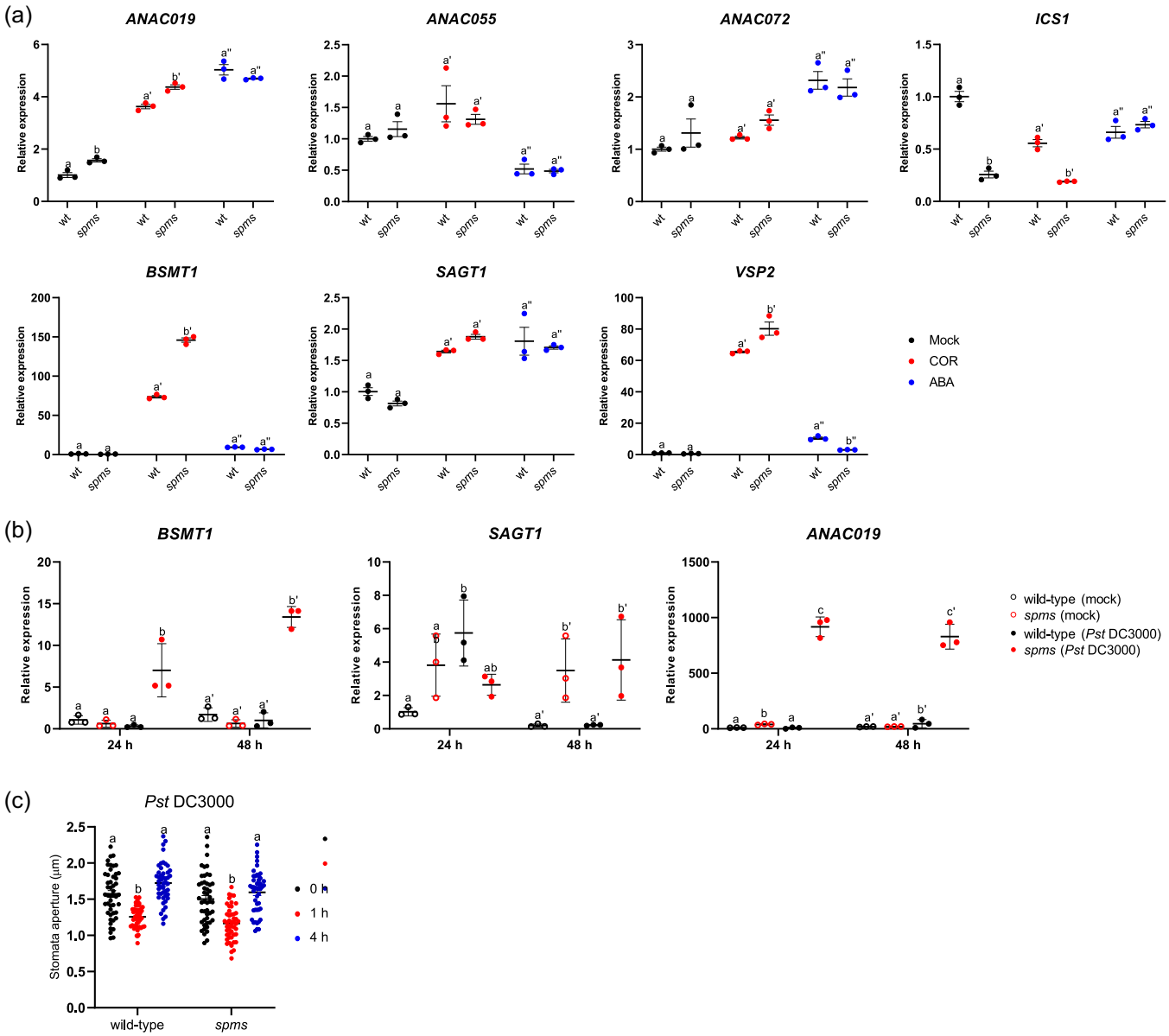

FIGURE 8 (a) Quantitative reverse-transcription polymerase chain reaction (qRT-PCR) expression analyses of *ANAC019*, *ANAC055* and *ANAC072*, SA metabolism genes (*ICS1*, *BSMT1* and *SAGT1*), and JA-responsive *VSP2* in wild type and *spermine synthase* (*spms*) treated with 1 μM coronatine (COR), 5 μM abscisic acid (ABA) or water (mock). Samples were harvested at 24 h of treatment. (b) qRT-PCR expression analyses of *BSMT1*, *SAGT1* and *ANAC019* in wild type and *spms* at 24 and 48 h of *Pst* DC3000 and mock (10 mM $MgCl_2$) inoculation. Expression values are relative to the wild-type (mock) treatment and represent the mean ± SD from three biological replicates per point of analysis. (c) Measurement of stomata aperture in leaf peels of wild-type and *spms* at 0, 1 and 4 h of *Pst* DC3000 treatment. [Color figure can be viewed at wileyonlinelibrary.com]

3.9 | Untargeted lipidomics analysis of *spms*

To further investigate the relationship between Spm deficiency and lipid metabolism, an untargeted lipidomics analysis was performed to identify differentially accumulating lipids between the *spms* mutant and wild-type plants under basal conditions. A total of 193 lipids could be identified (Supporting Information: Table S5), which were assigned to various lipid classes, including glycerophospholipids (representing 69% in the wild-type), sphingolipids (13%), galactolipids (9.5%), sterol lipids (6.7%), prenol lipids (1.4%) and glycerolipids (0.21%) (Figure 10a). Most lipid classes showed similar levels between the *spms* mutant and wild-type, except for galactolipids, most predominant lipids in thylakoid membranes of chloroplasts, which exhibited significant accumulation in *spms* (12.9%) (Figure 10a). Detailed examination of galactolipid subclasses revealed a significant increase in the levels of MGDG (18:3, 16:3), MGDG (18:3, 16:2), and monogalactosylmonoacylglycerol (MGMG) (16:3) in the *spms* mutant compared with the wild type (Figure 10b).

α-LeA (C18:3) derived from MGDG serves as the principal substrate for JA biosynthesis (Li & Yu, 2018; Lin et al., 2016). In the

digalactosyldiacylglycerol synthase 1 (*dgd1*) mutant, characterized by increased MGDG to digalactosyldiacylglycerol (DGDG) ratio due to impaired MGDG to DGDG conversion, there is a notable elevation in JA production even under basal conditions (Lin et al., 2016). This observation suggests that the augmented availability of MGDG in *spms*, as compared with wild-type plants, may contribute to the enhanced biosynthesis of JA. Collectively, these findings substantiate the specific impact of Spm deficiency on galactolipid metabolism, leading to the accumulation of MGDG and MGMG containing unsaturated C16 fatty acids and a greater pool of α-LeA (C18:3) that can be used as precursor for JA biosynthesis.

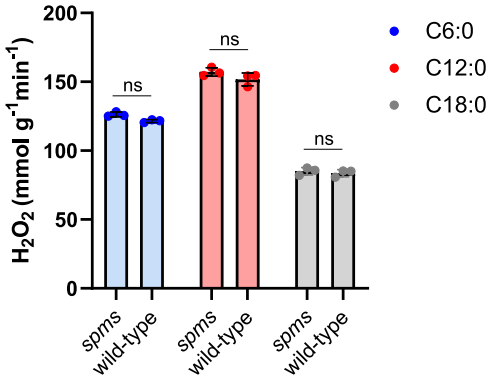

FIGURE 9 Measurement of Acyl-CoA oxidase activity. Acyl-CoA oxidase activity assays in 3-day-old wild-type and *spermine synthase* (*spms*) seedlings using *n*-hexanoyl-CoA (C6:0), lauroyl-CoA (C12:0) and stearoyl-CoA (C18:0) as substrates. Values represent the mean ± SD from three biological replicates. Ns, not significant according to Student's *t* test. [Color figure can be viewed at wileyonlinelibrary.com]

3.10 | Spm deficiency enhances disease resistance to *B. cinerea*

As the *spms* mutant already displayed higher JA levels than the wild type under basal conditions, we aimed to investigate the disease resistance phenotypes to the necrotrophic fungal pathogen *B. cinerea*. To accomplish this, we measured the lesion size induced by droplet inoculation of *B. cinerea* on leaves of both *spms* and wild-type plants (Ferrari et al., 2003), and determined fungal growth by real-time quantification at 24 and 48 h of spray inoculation (Gachon & Saindrenan, 2004). Compared with *spms*, the wild type exhibited larger lesion formation (Figure 11a) and higher fungal growth determined by qPCR quantification of *B. cinerea* and Arabidopsis DNA using specific primers for *β-tubuline* and *Actin2*, respectively (Figure 11b). The data indicated that Spm deficiency triggers greater resistance to *B. cinerea* infection compared with wild-type plants. Quantification of polyamine levels in wild-type plants inoculated with *B. cinerea* revealed a significant raise in Put and decline in Spm levels after 48 h of treatment (Figure 11c). Overall, the data indicated that *B. cinerea* infection leads to a decrease in Spm levels, and the absence of Spm results in increased resistance to the pathogen.

3.11 | Spm alleviates ER stress during *Pst* DC3000 infection

In addition to the effect of Spm deficiency on JA and SA-mediated defence responses to *Pst* DC3000, RNA-seq data also pointed to a potential contribution of Spm in mitigating ER stress (Figure 3). The ER is an important organelle that performs various functions, including the proper folding and processing of proteins. Accumulation of unfolded or misfolded proteins triggers a stress response within

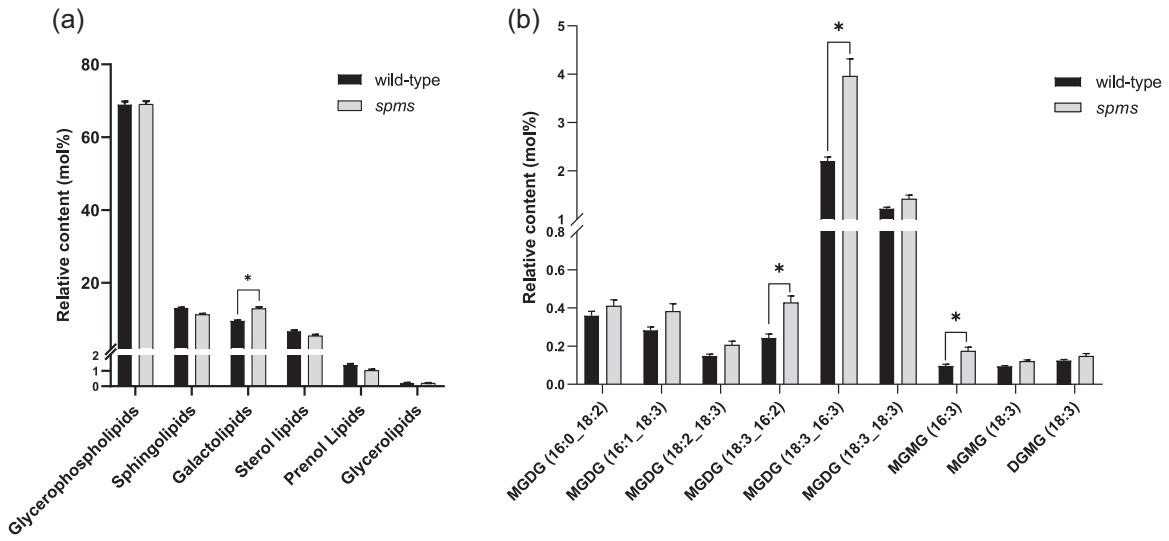

FIGURE 10 (a) Relative content of main lipid classes and (b) major galactolipids subclasses identified by ultra-performance-mass spectrometry untargeted lipidomics analysis in 5-week-old *spermine synthase* (*spms*) and wild-type plants under basal conditions. Asterisks indicate significant differences according to Student's *t* test (*$p < 0.05$, **$p < 0.01$).

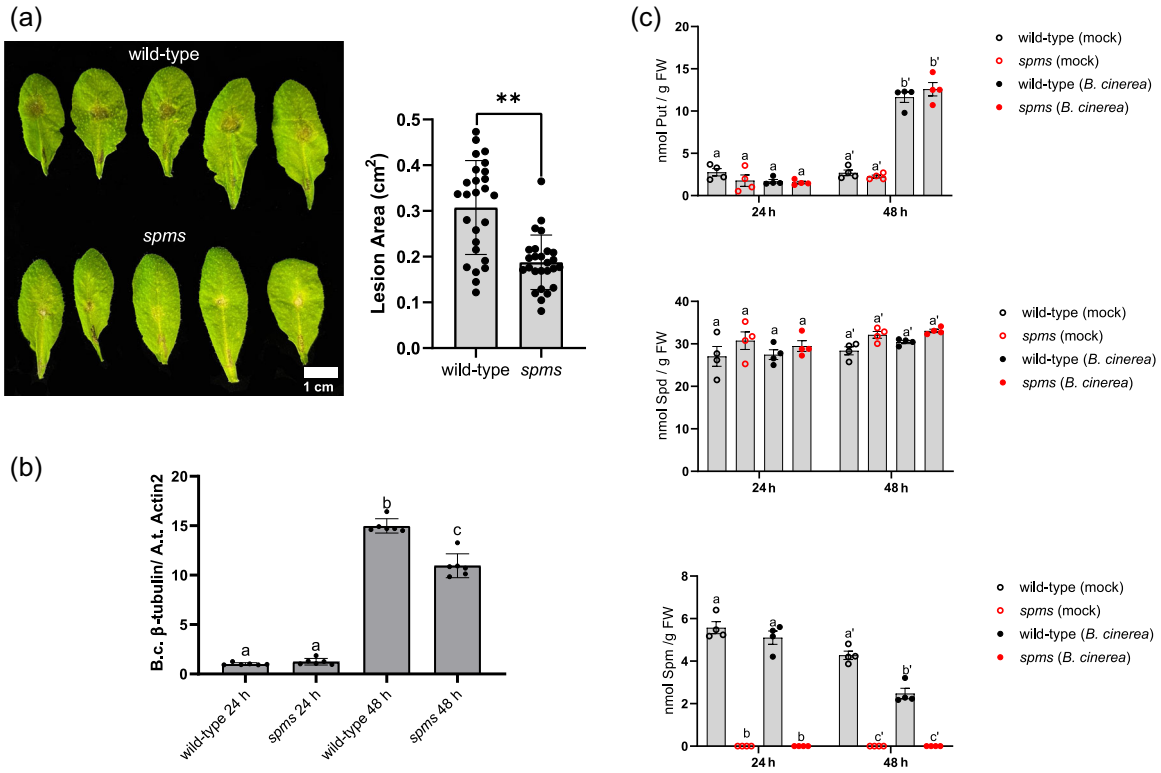

FIGURE 11 (a) Disease resistance phenotypes to *B. cinerea* infection in 5-week-old *spermine synthase* (*spms*) and wild-type plants determined by measurement of lesion size induced by droplet inoculation (4×10^6 spores mL^{-1}) at 72 h of treatment. (b) Real-time quantification of the relative abundance of *B. cinerea* (*B.c.*) and *A. thaliana* (*A.t.*) DNA at 24 h and 48 h of spray inoculation (5×10^5 spores mL^{-1}), using specific primers for *β-tubuline* (*B.c.*) and *Actin2* (*A.t.*). (c) Concentrations of free putrescine (Put), spermidine (Spd) and spermine (Spm) at 24 and 48 h of *B. cinerea* (5×10^5 spores mL^{-1}) and mock (Gamborg's B5 medium with 2% sucrose) spray inoculation in the wild type. Different letters indicate significant differences ($p < 0.05$) according to two-way analysis of variance followed by Tukey's posthoc test. [Color figure can be viewed at wileyonlinelibrary.com]

the ER, which is known as the unfolded protein response (UPR) (Pastor-Cantizano et al., 2020; Yu et al., 2022). To further investigate the potential contribution of Spm to ER stress avoidance, we determined the expression of known ER stress responsive genes in *spms* and wild-type plants at 24 and 48 h of bacteria and mock inoculation (Figure 12a). In response to *Pst* DC3000, the biomarkers for UPR activation *BIP3*, *PDIL1-1* and spliced-*bZIP60* (*sbZIP60*) were more strongly induced in *spms* than in the wild-type. Furthermore, treatment with the ER stress-trigger TM that inhibits N-linked glycosylation of proteins also led to stronger upregulation of these genes in *spms* compared with the wild-type (Figure 12b). However, treatment of wild-type seedlings with TM did not elicit significant changes in polyamine levels compared with the mock treatment (Figure 12c). Root growth inhibition assays were consistent with the gene expression data and indicated that the *spms* mutant was more sensitive to TM than the wild type (Figure 12d). The data indicated that Spm is required to alleviate ER stress during *Pst* DC3000 infection. When treated with various compounds that induce ER stress, such as BFA, which disrupts the structure and function of the Golgi apparatus, or DTT, which interferes with disulfide bonds and proper protein folding, the biosynthesis of Put was stimulated (Supporting Information: Figure S9). These findings suggest that polyamine metabolism responds to specific ER-stress-inducing agents, potentially due to variations in their underlying mechanisms.

4 | DISCUSSION

In this work, we report that Spm deficiency shifts the balance between JA and SA responses, by stimulating JA biosynthesis and dampening SA responses. This leads to enhanced disease resistance to the necrotrophic fungal pathogen *B. cinerea* and susceptibility to spray inoculated *Pst* DC3000. SARD1 and CBP60g are members of the CBP60 family of plant-specific transcription factors that play a direct role in regulating SA metabolism during defence. Transcription of key genes involved in SA biosynthesis *ICS1*, *EDS5* and *PBS3* is coordinately regulated by SARD1 and CBP60g (Sun et al., 2015; Wang et al., 2009, 2011; Zhang et al., 2010). Through RNA-seq and further qRT-PCR expression analyses, we found that transcripts of *SARD1* and *CBP60g*, as well as *ICS1*, *EDS5*, *PBS3* and other SA and SAR-related genes were more strongly upregulated in wild type than Spm-deficient (*spms*) plants in response to *Pst* DC3000 (Figure 4a,b). Consistent with this, SA accumulated significantly less in *spms* than in wild-type plants at 48 h of *Pst* DC3000 treatment (Figure 4c). The

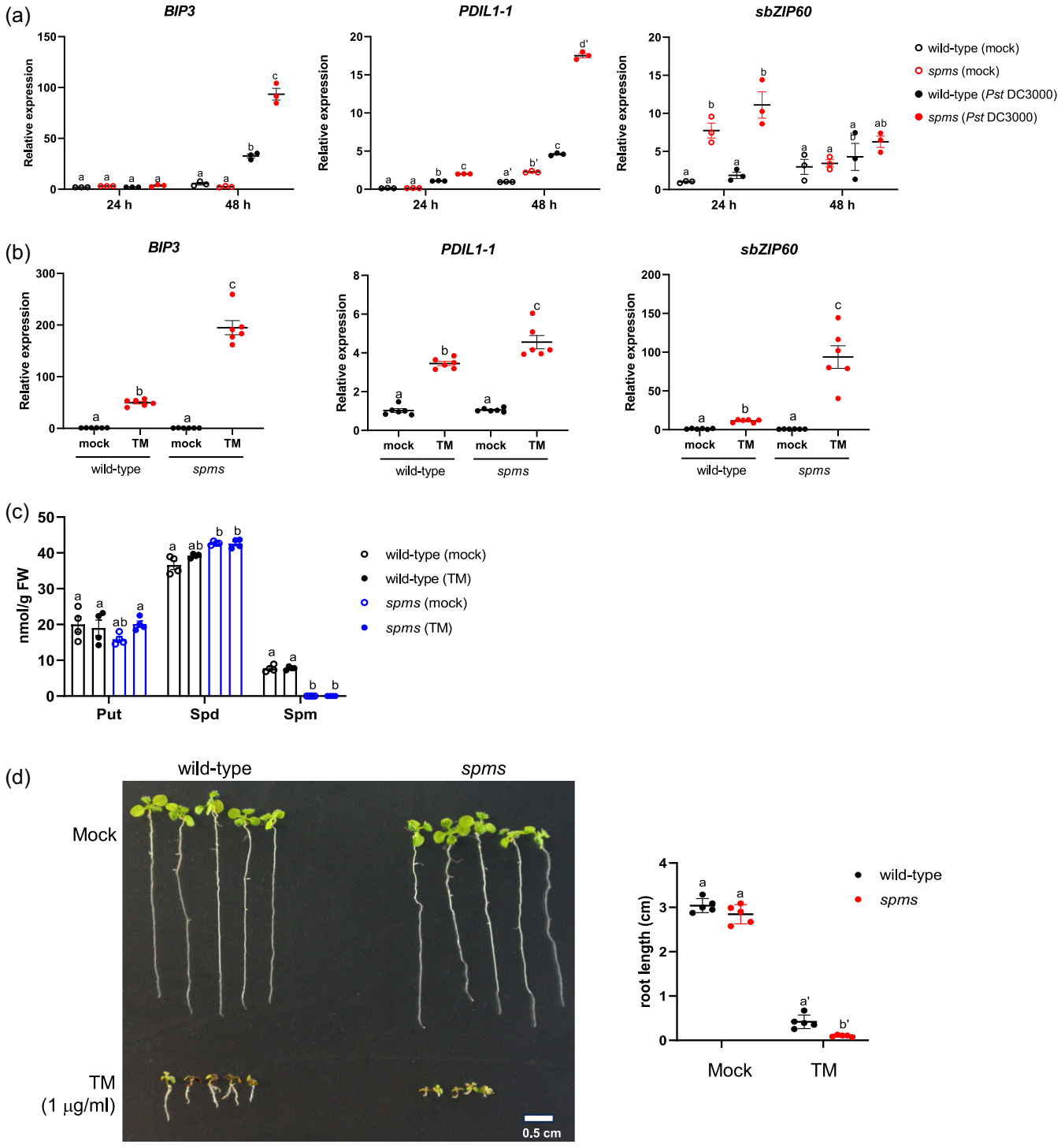

FIGURE 12 Effect of Spm deficiency on ER stress. Quantitative reverse-transcription polymerase chain reaction (qRT-PCR) expression analyses of *BIP3*, *PDIL1-1* and spliced-*bZIP60* (*sbZIP60*) in *spms* and wild-type plants at (a) 24 and 48 h of *Pst* DC3000 (OD_{600} = 0.001) and mock (10 mM $MgCl_2$) infiltration and (b) at 6 h of tunicamycin (1 μg mL^{-1}, TM) and mock treatment. Expression values are relative to the wild-type (mock) treatment and represent the mean ± SD from three to six biological replicates per point of analysis. (c) Polyamine levels in *spms* and wild-type seedlings at 24 h of 1 μg mL^{-1} TM treatment. (d) Root growth phenotypes of *spms* and wild-type seedlings grown in the presence of TM or mock. Values represent the mean ± SD from the indicated biological replicates per point of analysis. Different letters indicate significant differences ($p < 0.05$) according to two-way analysis of variance followed by Tukey's posthoc test. [Color figure can be viewed at wileyonlinelibrary.com]

data indicated that Spm deficiency compromises SA biosynthesis and the defence response to *Pst* DC3000.

Interestingly, when *Pst* DC3000 was directly infiltrated into the intercellular leaf space, there were no significant differences in the growth rate of *Pst* DC3000 between the *spms* mutant and the wild type (Zhang et al., 2023). The distinct disease resistance in response to spray or leaf infiltration has also been documented in the *fls2* mutant (Zipfel et al., 2004) and likely reflects differences in the capacity of the bacteria to reach the intercellular leaf space of the host tissue and propagate under more natural conditions (Melotto et al., 2006).

Spm-deficient plants contained higher levels of JA, JA-Ile and OPDA under basal conditions and during the defence response to *Pst* DC3000 (Figure 7). They also showed enhanced JA/COR responses (Supporting Information: Figure S6) in correlation with increased *LOX2*, *LOX3*, *AOC1*, *OPR3*, *OPCL1*, *MYC2*, *JAZ1*, *JAZ10*, *VSP1* and *VSP2* expression at 48 h of *Pst* DC3000 inoculation, and AOC2 protein abundance already under basal conditions (Figures 5 and 6, and Supporting Information: Table S4.1). It has been reported that the coordinated action of *ANAC019*, *ANAC055* and *ANAC072* mediates JA responses and COR-induced suppression of SA accumulation. The latter is achieved by repressing *ICS1* and activating *BSMT1* expression, leading to a shift in SA metabolism dynamics that contributes to JA-SA antagonism and bacterial virulence (Bu et al., 2008; Zheng et al., 2012). The stimulation of JA biosynthesis and signalling in *spms* might contribute to the dampening of SA responses through JA-SA antagonism (Hou & Tsuda, 2022). In agreement with this, the expression of *ANAC019* and its target genes *ICS1* and *BSMT1* were more strongly deregulated in *spms* than in the wild-type in response to *Pst* DC3000 and COR (Figure 8a,b).

By employing shotgun lipidomics, we observed a significant increase in the levels of MGDG (18:3, 16:3), MGDG (18:3, 16:2) and MGMG (16:3) in Spm-deficient compared with wild-type plants (Figure 10b). As MGDG serves as a primary precursor for JA biosynthesis (Li & Yu, 2018; Lin et al., 2016), the elevated levels of MGDG levels could enhance the availability of α-LeA (C18:3), used as substrate of plastidial 13-LOX. The *spms* mutant also showed enhanced disease resistance to *B. cinerea* compared with wild-type plants. Our results are consistent with previous reports that suggest polyamines may facilitate the growth of certain necrotrophic pathogens through additional potential interactions with the ethylene pathway and ROS production (Marina et al., 2008; Nambeesan et al., 2012; Rea et al., 2002).

Chromatin immunoprecipitation sequencing identified the promoters of *ADC1*, *ADC2* and *SAMDC1* as potential targets of SARD1, suggesting a coordination of polyamine and SA pathways (Sun et al., 2015). However, we found that Put accumulation triggered by *Pst* DC3000 was not compromised but stimulated in *eds1*, *sid2-1* and *npr1-1* mutants, thus being an SA-independent response (Figure S2). In contrast, Put increases triggered by *Pst* DC3000 were significantly reduced in *coi1-1* and *myc2* mutants (Supporting Information: Figure S2), indicating an important contribution of JA signalling in modulating Put metabolism in *Arabidopsis*. The modulation of polyamine metabolism by JA has been observed in various species. In *Hyosciamus muticus*, MeJA treatment triggers an increase in the levels of Put, as well as Spd and Spm to a lesser extent (Biondi et al., 2000). In *Zea mays*, the expression and activity of the PAO enzyme, ZmPAO, are induced by wounding and MeJA treatment, resulting in higher levels of ROS, lignin, and suberin deposition that are required for wound healing (Angelini et al., 2008). In *Nicotiana attenuata*, the biosynthesis of polyamines conjugated to phenolic compounds (phenolamides) is triggered by herbivore attack and is associated with increased JA and LOX3 activity (Onkokesung et al., 2012). Similarly, in tomato, MYC1 and MYC2 play a role in the JA-mediated activation of phenolamide biosynthesis (Swinnen et al., 2022). In *Arabidopsis*, *N-acetyltransferase 1* (*NATA1*), which acetylates Put, is upregulated in response to COR, leading to a reduction in free Put levels and enhanced disease susceptibility to *Pst* DC3000 (Lou et al., 2016). Taken together, these findings indicate that JA and the bacterial phytotoxin COR can reshape polyamine metabolism in different plant species.

In addition to an impact on JA-SA balance, we found that Spm deficiency enhanced ER stress in response to *Pst* DC3000. The ER is an essential organelle for phospholipid synthesis, Ca^{2+} storage and the synthesis and folding of proteins. During cellular stress, the protein folding capacity of the ER can be compromised, leading to the accumulation of misfolded or unfolded proteins in the ER lumen. This triggers a cellular response, known as the UPR, to restore net protein folding capacity by increased ER chaperone production, upregulation of lipid synthesis and repression of translation (Pastor-Cantizano et al., 2020; Yu et al., 2022). We found increased expression of UPR biomarkers *BIP3*, *sbZIP60* and *PDIL1-1* in *spms* mutant relative to the wild type during *Pst* DC3000 infection, and in response to TM treatment (Figure 12a,b). In agreement with a potential effect of Spm buffering ER stress, *spms* was more sensitive to TM than the wild type (Figure 12d). Even though the treatment with TM did not result in any significant changes in polyamine contents relative to the mock treatment (Figure 12c), other ER-stress-inducing compounds such as BFA and DTT triggered changes in polyamine homoeostasis. This is likely attributed to their different underlying mechanisms in triggering ER stress (Supporting Information: Figure S9). Deregulation of Spm homoeostasis by *SPMS* overexpression also triggers transcriptional responses compatible with ER stress in *Arabidopsis*, such as upregulation of UPR biomarker genes *bZIP17*, *bZIP28* and *BIP3*. This response, which was dependent on Ca^{2+} signalling, suggested an effect of Spm on Ca^{2+} homoeostasis in the ER (Sagor et al., 2015; Zhang et al., 2023). The involvement of Spm in buffering ER stress responses has also been reported in *Magnaporthe oryzae*, the blast fungus responsible for rice blast disease. In this case, Spm plays a crucial role in pathogenicity by ensuring a secure seal of the appressorium on the host leaf surface by facilitating the production of mucilage, which is rich in glycoproteins. In this context, Spm acts as ROS scavenger, buffering NADPH oxidase-1-generated oxidative stress in the ER lumen and preventing ER stress and mucilage production (Rocha et al., 2020). Collectively, an imbalance in Spm levels during stress conditions could disrupt Ca^{2+} and ROS homoeostasis in the ER, potentially leading to ER stress and UPR activation.

In summary, our study provides evidence that Spm deficiency potentiates JA biosynthesis influencing SA dynamics, *Pst* DC3000

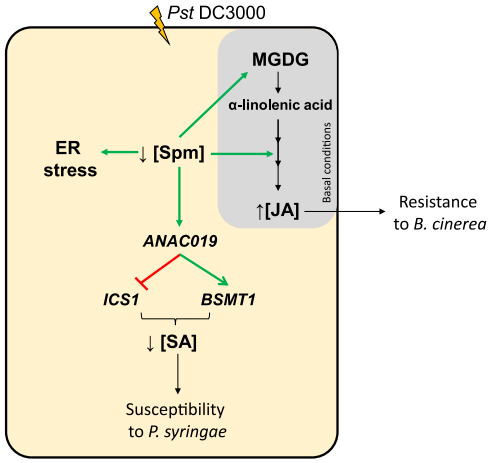

FIGURE 13 Mechanistic model for the influence of spermine (Spm) on the modulation of salicylic acid (SA) and jasmonic acid (JA) defence responses. Spm deficiency results in increased levels of monogalactosyldiacylglycerol (MGDG) and increased expression of JA biosynthesis genes that correlate with elevated levels of JA under basal conditions and in response to *Pst* DC3000. Spm deficiency enhances *ANAC019* expression in response to *Pst* DC3000, leading to a more robust deregulation of SA-metabolism genes *ICS1* and *BSMT1*, and reduced SA content. This way, Spm deficiency shifts the balance between JA and SA, which associates with enhanced susceptibility to *Pst* DC3000 and disease resistance to *B. cinerea*. Spm deficiency also triggers endoplasmic reticulum (ER) stress signalling in response to *Pst* DC3000, which indicates the importance of this polyamine in alleviating ER stress during defence. [Color figure can be viewed at wileyonlinelibrary.com]

and *B. cinerea* disease resistance, and exacerbating ER stress in response to the bacteria (Figure 13).

ACKNOWLEDGEMENTS

This work was financially supported by the grants: PID2021-126896OB-I00 funded by Ministerio de Ciencia e Innovación MCIN/Agencia Estatal de Investigación AEI/10.13039/501100011033 (Spain) and by the "European Regional Development Fund (ERDF) a way of making Europe"; PDC2021-121267-I00 funded by Ministerio de Ciencia e Innovación MCIN/Agencia Estatal de Investigación AEI/10.13039/501100011033 (Spain) and European Union Next GenerationEU/PRTR. A.G-C. acknowledges support from Generalitat Valenciana (CIAICO/2021/063). C.Z., J.Z. and C.D. acknowledge support from the CSC (China Scholarship Council) for funding their doctoral fellowship. E.M. is holder of the grant PRE2018-083289 funded by MCIN/AEI/10.13039/501100011033 and by "European Social Fund Investing in your future".

CONFLICT OF INTEREST STATEMENT

The authors declare no conflict of interest.

DATA AVAILABILITY STATEMENT

All data supporting the findings of this study are available within the paper and within its Supporting Information published online. The RNA-seq data have been deposited to ArrayExpress (https://www.ebi.ac.uk/arrayexpress/) under the accession identifier E-MTAB-13086. The mass spectrometry proteomics data have been deposited to the ProteomeXchange Consortium via the PRIDE (https://www.ebi.ac.uk/pride/) partner repository with the data set identifier PXD041901.

ORCID

Aurelio Gómez-Cadenas http://orcid.org/0000-0002-4598-2664
Rubén Alcázar http://orcid.org/0000-0002-3567-7586

REFERENCES

Adham, A.R., Zolman, B.K., Millius, A. & Bartel, B. (2005) Mutations in *Arabidopsis* acyl-CoA oxidase genes reveal distinct and overlapping roles in β-oxidation. *The Plant Journal*, 41, 859–874.

Al-Habsi, M., Chamoto, K., Matsumoto, K., Nomura, N., Zhang, B., Sugiura, Y. et al. (2022) Spermidine activates mitochondrial trifunctional protein and improves antitumor immunity in mice. *Science*, 378, eabj3510.

Andreou, A. & Feussner, I. (2009) Lipoxygenases–structure and reaction mechanism. *Phytochemistry*, 70, 1504–1510.

Angelini, R., Tisi, A., Rea, G., Chen, M.M., Botta, M., Federico, R. et al. (2008) Involvement of polyamine oxidase in wound healing. *Plant Physiology*, 146, 162–177.

Attaran, E., Zeier, T.E., Griebel, T. & Zeier, J. (2009) Methyl salicylate production and jasmonate signaling are not essential for systemic acquired resistance in *Arabidopsis*. *The Plant Cell*, 21, 954–971.

Biondi, S., Fornalé, S., Oksman-Caldentey, K.M., Eeva, M., Agostani, S. & Bagni, N. (2000) Jasmonates induce over-accumulation of methylputrescine and conjugated polyamines in *Hyoscyamus muticus* L. root cultures. *Plant Cell Reports*, 19, 691–697.

Brooks, D.M., Bender, C.L. & Kunkel, B.N. (2005) The *Pseudomonas syringae* phytotoxin coronatine promotes virulence by overcoming salicylic acid-dependent defences in *Arabidopsis thaliana*. *Molecular Plant Pathology*, 6, 629–639.

Bu, Q., Jiang, H., Li, C.-B., Zhai, Q., Zhang, J., Wu, X. et al. (2008) Role of the *Arabidopsis thaliana* NAC transcription factors ANAC019 and ANAC055 in regulating jasmonic acid-signaled defense responses. *Cell Research*, 18, 756–767.

Cao, H., Glazebrook, J., Clarke, J.D., Volko, S. & Dong, X. (1997) The *Arabidopsis NPR1* gene that controls systemic acquired resistance encodes a novel protein containing ankyrin repeats. *Cell*, 88, 57–63.

Carbon, S., Douglass, E., Dunn, N., Good, B., Harris, N.L., Lewis, S.E. et al. (2019) The Gene Ontology resource: 20 years and still GOing strong. *Nucleic Acids Research*, 47, D330–D338.

Castillo, M.C., Martínez, C., Buchala, A., Métraux, J.-P. & León, J. (2004) Gene-specific involvement of β-oxidation in wound-activated responses in *Arabidopsis*. *Plant Physiology*, 135, 85–94.

Cheng, C.Y., Krishnakumar, V., Chan, A.P., Thibaud-Nissen, F., Schobel, S. & Town, C.D. (2017) Araport11: a complete reannotation of the *Arabidopsis thaliana* reference genome. *The Plant Journal*, 89, 789–804.

Chini, A., Fonseca, S., Fernández, G., Adie, B., Chico, J.M., Lorenzo, O. et al. (2007) The JAZ family of repressors is the missing link in jasmonate signalling. *Nature*, 448, 666–671.

Cuevas, J.C., López-Cobollo, R., Alcázar, R., Zarza, X., Koncz, C., Altabella, T. et al. (2008) Putrescine is involved in *Arabidopsis* freezing tolerance and cold acclimation by regulating abscisic acid levels in response to low temperature. *Plant Physiology*, 148, 1094–1105.

Cui, J., Bahrami, A.K., Pringle, E.G., Hernandez-Guzman, G., Bender, C.L., Pierce, N.E. et al. (2005) *Pseudomonas syringae* manipulates systemic plant defenses against pathogens and herbivores. *Proceedings of the National Academy of Sciences*, 102, 1791–1796.

Dean, J.V. & Delaney, S.P. (2008) Metabolism of salicylic acid in wild-type, *ugt74f1* and *ugt74f2* glucosyltransferase mutants of *Arabidopsis thaliana*. *Physiologia Plantarum*, 132, 417–425.

Dongus, J.A. & Parker, J.E. (2021) EDS1 signalling: at the nexus of intracellular and surface receptor immunity. *Current Opinion in Plant Biology*, 62, 102039.

Dunn, W.B., Broadhurst, D., Begley, P., Zelena, E., Francis-McIntyre, S., Anderson, N. et al. (2011) Human Serum Metabolome (HUSERMET) Consortium. Procedures for large-scale metabolic profiling of serum and plasma using gas chromatography and liquid chromatography coupled to mass spectrometry. *Nature Protocols*, 6, 1060–1083.

Fan, G., Yang, Y., Li, T., Lu, W., Du, Y., Qiang, X. et al. (2018) A *Phytophthora capsici* RXLR effector targets and inhibits a plant PPIase to suppress endoplasmic reticulum-mediated immunity. *Molecular Plant*, 11, 1067–1083.

Ferrari, S., Plotnikova, J.M., De Lorenzo, G. & Ausubel, F.M. (2003) Arabidopsis local resistance to *Botrytis cinerea* involves salicylic acid and camalexin and requires EDS4 and PAD2, but not SID2, EDS5 or PAD4. *The Plant Journal*, 35, 193–205.

Feys, B.J., Moisan, L.J., Newman, M.A. & Parker, J.E. (2001) Direct interaction between the *Arabidopsis* disease resistance signaling proteins, EDS1 and PAD4. *The EMBO Journal*, 20, 5400–5411.

Feys, B.J., Wiermer, M., Bhat, R.A., Moisan, L.J., Medina-Escobar, N., Neu, C. et al. (2005) *Arabidopsis* SENESCENCE-ASSOCIATED GENE101 stabilizes and signals within an ENHANCED DISEASE SUSCEPTIBILITY1 complex in plant innate immunity. *The Plant Cell*, 17, 2601–2613.

Feys, B.J.F., Benedetti, C.E., Penfold, C.N. & Turner, J.G. (1994) Arabidopsis mutants selected for resistance to the phytotoxin coronatine are male sterile, insensitive to methyl jasmonate, and resistant to a bacterial pathogen. *The Plant Cell*, 6, 751–759.

Gachon, C. & Saindrenan, P. (2004) Real-time PCR monitoring of fungal development in *Arabidopsis thaliana* infected by *Alternaria brassicicola* and *Botrytis cinerea*. *Plant Physiology and Biochemistry*, 42, 367–371.

Garcion, C., Lohmann, A., Lamodière, E., Catinot, J., Buchala, A., Doermann, P. et al. (2008) Characterization and biological function of the *ISOCHORISMATE SYNTHASE2* gene of *Arabidopsis*. *Plant Physiology*, 147, 1279–1287.

Gerhardt, B. (1987) Peroxisomes and fatty acid degradation, *Methods in Enzymology. Plant Cell Membranes*. Academic Press, pp. 516–525.

Gerlin, L., Baroukh, C. & Genin, S. (2021) Polyamines: double agents in disease and plant immunity. *Trends in Plant Science*, 26, 1061–1071.

Glazebrook, J. (2005) Contrasting mechanisms of defense against biotrophic and necrotrophic pathogens. *Annual Review of Phytopathology*, 43, 205–227.

Goepfert, S. & Poirier, Y. (2007) β-Oxidation in fatty acid degradation and beyond. *Current Opinion in Plant Biology*, 10, 245–251.

Gonzalez, M.E., Marco, F., Minguet, E.G., Carrasco-Sorli, P., Blázquez, M.A. & Carbonell, J. et al. (2011) Perturbation of spermine synthase gene expression and transcript profiling provide new insights on the role of the tetraamine spermine in *Arabidopsis* defense against *Pseudomonas viridiflava*. *Plant Physiology*, 156, 2266–2277.

Di Guida, R., Engel, J., Allwood, J.W., Weber, R.J.M., Jones, M.R., Sommer, U. et al. (2016) Non-targeted UHPLC-MS metabolomic data processing methods: a comparative investigation of normalisation, missing value imputation, transformation and scaling. *Metabolomics*, 12, 93.

Hayashi, M., Toriyama, K., Kondo, M., Nishimura, M., Hayashi, M., Toriyama, K. et al. (1998) 2,4-Dichlorophenoxybutyric acid-resistant mutants of *Arabidopsis* have defects in glyoxysomal fatty acid b-oxidation. *The Plant Cell*, 10, 183–195.

Hou, S. & Tsuda, K. (2022) Salicylic acid and jasmonic acid crosstalk in plant immunity. *Essays in Biochemistry*, 66, 647–656.

Hryb, D.J. & Hogg, J.F. (1979) Chain length specificities of peroxisomal and mitochondrial β-oxidation in rat liver. *Biochemical and Biophysical Research Communications*, 87, 1200–1206.

Hu, J., Baker, A., Bartel, B., Linka, N., Mullen, R.T., Reumann, S. et al. (2012) Plant peroxisomes: biogenesis and function. *The Plant Cell*, 24, 2279–2303.

Ishiguro, S., Kawai-Oda, A., Ueda, J., Nishida, I. & Okada, K. (2001) The DEFECTIVE IN ANTHER DEHISCENCE1 gene encodes a novel phospholipase A1 catalyzing the initial step of jasmonic acid biosynthesis, which synchronizes pollen maturation, anther dehiscence, and flower opening in *Arabidopsis*. *The Plant Cell*, 13, 2191–2209.

Kloek, A.P., Verbsky, M.L., Sharma, S.B., Schoelz, J.E., Vogel, J., Klessig, D.F. et al. (2001) Resistance to *Pseudomonas syringae* conferred by an *Arabidopsis thaliana* coronatine-insensitive (coi1) mutation occurs through two distinct mechanisms: disease resistance in an *A. thaliana* COI1 mutant. *The Plant Journal*, 26, 509–522.

Li, H. & Yu, C.-W. (2018) Chloroplast galactolipids: the link between photosynthesis, chloroplast shape, jasmonates, phosphate starvation and freezing tolerance. *Plant and Cell Physiology*, 59, 1128–1134.

Li, M., Yu, G., Cao, C. & Liu, P. (2021) Metabolism, signaling, and transport of jasmonates. *Plant Communications*, 2, 100231.

Lin, Y.-T., Chen, L.-J., Herrfurth, C., Feussner, I. & Li, H. (2016) Reduced biosynthesis of digalactosyldiacylglycerol, a major chloroplast membrane lipid, leads to oxylipin overproduction and phloem cap lignification in *Arabidopsis*. *The Plant Cell*, 28, 219–232.

Liu, C., Atanasov, K.E., Arafaty, N., Murillo, E., Tiburcio, A.F., Zeier, J. et al. (2020a) Putrescine elicits ROS-dependent activation of the salicylic acid pathway in *Arabidopsis thaliana*. *Plant, Cell and Environment*, 43, 2755–2768.

Liu, C., Atanasov, K.E., Tiburcio, A.F. & Alcázar, R. (2019) The polyamine putrescine contributes to H2O2 and RbohD/F-dependent positive feedback loop in *Arabidopsis* PAMP-triggered immunity. *Frontiers in Plant Science*, 10, 894.

Liu, Y., Sun, T., Sun, Y., Zhang, Y., Radojičić, A., Ding, Y. et al. (2020b) Diverse roles of the salicylic acid receptors NPR1 and NPR3/NPR4 in plant immunity. *The Plant Cell*, 32, 4002–4016.

Livak, K.J. & Schmittgen, T.D. (2001) Analysis of relative gene expression data using real-time quantitative PCR and the $2^{-\Delta\Delta CT}$ method. *Methods*, 25, 402–408.

Lorenzo, O., Chico, J.M., Saénchez-Serrano, J.J. & Solano, R. (2004) JASMONATE-INSENSITIVE1 encodes a MYC transcription factor essential to discriminate between different jasmonate-regulated defense responses in *Arabidopsis*. *The Plant Cell*, 16, 1938–1950.

Lou, Y.-R., Bor, M., Yan, J., Preuss, A.S. & Jander, G. (2016) Arabidopsis NATA1 acetylates putrescine and decreases defense-related hydrogen peroxide accumulation. *Plant Physiology*, 171, 1443–1455.

Ma, S.-W., Morris, V. L. & Cuppels, D.A. (1991) Characterization of a DNA region required for production of the phytotoxin coronatine by *Pseudomonas syringae* pv. *tomato*. *Molecular Plant-Microbe Interactions*, 4, 69–74.

Marco, F., BusÃ³, E. & Carrasco, P. (2014) Overexpression of *SAMDC1* gene in *Arabidopsis thaliana* increases expression of defense-related genes as well as resistance to *Pseudomonas syringae* and *Hyaloperonospora arabidopsidis*. *Frontiers in Plant Science*, 5, 115.

Marina, M., Maiale, S.J., Rossi, F., Romero, F., Rivas, E.I., Gárriz, A. et al. (2008) Apoplastic polyamine oxidation plays different roles in local responses of tobacco to infection by the necrotrophic fungus *Sclerotinia sclerotiorum* and the biotrophic bacterium *Pseudomonas viridiflava*. *Plant Physiology*, 147, 2164–2178.

Melotto, M., Underwood, W., Koczan, J., Nomura, K. & He, S.Y. (2006) Plant stomata function in innate immunity against bacterial invasion. *Cell*, 126, 969–980.

Mi, H., Muruganujan, A., Casagrande, J.T. & Thomas, P.D. (2013) Large-scale gene function analysis with the PANTHER classification system. *Nature Protocols*, 8, 1551–1566.

Mi, H., Muruganujan, A., Ebert, D., Huang, X. & Thomas, P.D. (2019) PANTHER version 14: more genomes, a new PANTHER GO-slim and improvements in enrichment analysis tools. *Nucleic Acids Research*, 47, D419–D426.

Mitsuya, Y., Takahashi, Y., Berberich, T., Miyazaki, A., Matsumura, H., Takahashi, H. et al. (2009) Spermine signaling plays a significant role in the defense response of *Arabidopsis thaliana* to cucumber mosaic virus. *Journal of Plant Physiology*, 166, 626–643.

Mittal, S. (1995) Role of the phytotoxin coronatine in the infection of *Arabidopsis thaliana* by *Pseudomonas syringae* pv. *tomato*. *Molecular Plant-Microbe Interactions*, 8, 165–171.

Mo, H., Wang, X., Zhang, Y., Yang, J. & Ma, Z. (2015) Cotton ACAULIS5 is involved in stem elongation and the plant defense response to *Verticillium dahliae* through thermospermine alteration. *Plant Cell Reports*, 34, 1975–1985.

Moschou, P.N., Sarris, P.F., Skandalis, N., Andriopoulou, A.H., Paschalidis, K.A., Panopoulos, N.J. et al. (2009) Engineered polyamine catabolism preinduces tolerance of tobacco to bacteria and oomycetes. *Plant Physiology*, 149, 1970–1981.

Nambeesan, S., AbuQamar, S., Laluk, K., Mattoo, A.K., Mickelbart, M.V., Ferruzzi, M.G. et al. (2012) Polyamines attenuate ethylene-mediated defense responses to abrogate resistance to *Botrytis cinerea* in tomato. *Plant Physiology*, 158, 1034–1045.

Nawrath, C., Heck, S., Parinthawong, N. & Métraux, J.-P. (2002) EDS5, an essential component of salicylic acid–dependent signaling for disease resistance in *Arabidopsis*, is a member of the MATE transporter family. *The Plant Cell*, 14, 275–286.

Nickstadt, A., Thomma, B.P.H.J., Feussner, I., Kangasjarvi, J., Zeier, J., Loeffler, C. et al. (2004) The jasmonate-insensitive mutant *jin1* shows increased resistance to biotrophic as well as necrotrophic pathogens. *Molecular Plant Pathology*, 5, 425–434.

Onkokesung, N., Gaquerel, E., Kotkar, H., Kaur, H., Baldwin, I.T. & Galis, I. (2012) MYB8 controls inducible phenolamide levels by activating three novel Hydroxycinnamoyl-Coenzyme A:Polyamine transferases in *Nicotiana attenuata*. *Plant Physiology*, 158, 389–407.

Pastor-Cantizano, N., Ko, D.K., Angelos, E., Pu, Y. & Brandizzi, F. (2020) Functional diversification of ER stress responses in *Arabidopsis*. *Trends in Biochemical Sciences*, 45, 123–136.

Peng, Y., Yang, J., Li, X. & Zhang, Y. (2021) Salicylic acid: biosynthesis and signaling. *Annual Review of Plant Biology*, 72, 761–791.

Rea, G., Metoui, O., Infantino, A., Federico, R. & Angelini, R. (2002) Copper amine oxidase expression in defense responses to wounding and *Ascochyta rabiei* invasion. *Plant Physiology*, 128, 865–875.

Rivals, I., Personnaz, L., Taing, L. & Potier, M.-C. (2007) Enrichment or depletion of a GO category within a class of genes: which test? *Bioinformatics*, 23, 401–407.

Rocha, R.O., Elowsky, C., Pham, N.T.T. & Wilson, R.A. (2020) Spermine-mediated tight sealing of the *Magnaporthe oryzae* appressorial pore-rice leaf surface interface. *Nature Microbiology*, 5, 1472–1480.

Sagor, G.H.M., Chawla, P., Kim, D.W., Berberich, T., Kojima, S., Niitsu, M. et al. (2015) The polyamine spermine induces the unfolded protein response via the MAPK cascade in *Arabidopsis*. *Frontiers in Plant Science*, 6, 687.

Sagor, G.H.M., Takahashi, H., Niitsu, M., Takahashi, Y., Berberich, T. & Kusano, T. (2012) Exogenous thermospermine has an activity to induce a subset of the defense genes and restrict cucumber mosaic virus multiplication in *Arabidopsis thaliana*. *Plant Cell Reports*, 31, 1227–1232.

Seo, S., Katou, S., Seto, H., Gomi, K. & Ohashi, Y. (2007) The mitogen-activated protein kinases WIPK and SIPK regulate the levels of jasmonic and salicylic acids in wounded tobacco plants. *The Plant Journal*, 49, 899–909.

Serrano, M., Wang, B., Aryal, B., Garcion, C., Abou-Mansour, E., Heck, S. et al. (2013) Export of salicylic acid from the chloroplast requires the multidrug and toxin extrusion-like transporter EDS5. *Plant Physiology*, 162, 1815–1821.

Sheard, L.B., Tan, X., Mao, H., Withers, J., Ben-Nissan, G., Hinds, T.R. et al. (2010) Jasmonate perception by inositol-phosphate-potentiated COI1–JAZ co-receptor. *Nature*, 468, 400–405.

Spoel, S.H., Koornneef, A., Claessens, S.M.C., Korzelius, J.P., Van Pelt, J.A., Mueller, M.J. et al. (2003) NPR1 modulates cross-talk between salicylate- and jasmonate-dependent defense pathways through a novel function in the cytosol. *The Plant Cell*, 15, 760–770.

Sun, T., Huang, J., Xu, Y., Verma, V., Jing, B., Sun, Y. et al. (2020) Redundant CAMTA transcription factors negatively regulate the biosynthesis of salicylic acid and N-hydroxypipecolic acid by modulating the expression of SARD1 and CBP60g. *Molecular Plant*, 13, 144–156.

Sun, T., Zhang, Y., Li, Y., Zhang, Q., Ding, Y. & Zhang, Y. (2015) ChIP-seq reveals broad roles of SARD1 and CBP60g in regulating plant immunity. *Nature Communications*, 6, 10159.

Swinnen, G., De Meyer, M., Pollier, J., Molina-Hidalgo, F.J., Ceulemans, E., Venegas-Molina, J. et al. (2022) The basic helix–loop–helix transcription factors MYC1 and MYC2 have a dual role in the regulation of constitutive and stress-inducible specialized metabolism in tomato. *New Phytologist*, 236, 911–928.

Takahashi, Y., Berberich, T., Miyazaki, A., Seo, S., Ohashi, Y. & Kusano, T. (2003) Spermine signalling in tobacco: activation of mitogen-activated protein kinases by spermine is mediated through mitochondrial dysfunction. *The Plant Journal*, 36, 820–829.

Takahashi, Y., Uehara, Y., Berberich, T., Ito, A., Saitoh, H., Miyazaki, A. et al. (2004) A subset of hypersensitive response marker genes, including HSR203J, is the downstream target of a spermine signal transduction pathway in tobacco. *The Plant Journal*, 40, 586–595.

Thines, B., Katsir, L., Melotto, M., Niu, Y., Mandaokar, A., Liu, G. et al. (2007) JAZ repressor proteins are targets of the SCFCOI1 complex during jasmonate signalling. *Nature*, 448, 661–665.

Tiburcio, A.F., Altabella, T., Bitrián, M. & Alcázar, R. (2014) The roles of polyamines during the lifespan of plants: from development to stress. *Planta*, 240, 1–18.

Wang, L., Tsuda, K., Sato, M., Cohen, J.D., Katagiri, F. & Glazebrook, J. (2009) *Arabidopsis* CaM binding protein CBP60g contributes to MAMP-induced SA accumulation and is involved in disease resistance against *Pseudomonas syringae*. *PLoS Pathogens*, 5, e1000301.

Wang, L., Tsuda, K., Truman, W., Sato, M., Nguyen, L.V., Katagiri, F. et al. (2011) CBP60g and SARD1 play partially redundant critical roles in salicylic acid signaling. *The Plant Journal*, 67, 1029–1041.

Wasternack, C. & Feussner, I. (2018) The oxylipin pathways: biochemistry and function. *Annual Review of Plant Biology*, 69, 363–386.

Wasternack, C. & Song, S. (2017) Jasmonates: biosynthesis, metabolism, and signaling by proteins activating and repressing transcription. *Journal of Experimental Botany*, 68, 1303–1321.

Wildermuth, M.C., Dewdney, J., Wu, G. & Ausubel, F.M. (2001) Isochorismate synthase is required to synthesize salicylic acid for plant defence. *Nature*, 414, 562–565.

Yu, C.-Y., Cho, Y., Sharma, O. & Kanehara, K. (2022) What's unique? The unfolded protein response in plants. *Journal of Experimental Botany*, 73, 1268–1276.

Zeng, W. & He, S.Y. (2010) A prominent role of the flagellin receptor FLAGELLIN-SENSING2 in mediating stomatal response to *Pseudomonas syringae* pv *tomato* DC3000 in *Arabidopsis*. *Plant Physiology*, 153, 1188–1198.

Zhang, C., Atanasov, K.E. & Alcázar, R. (2023) Spermine inhibits PAMP-induced ROS and Ca2+ burst and reshapes the transcriptional landscape of PAMP-triggered immunity in *Arabidopsis*. *Journal of Experimental Botany*, 74, 427–442.

Zhang, S., Klessig, D.F., Zhang, S. & Klessig, D.F. (1997) Salicylic acid activates a 48-kD MAP kinase in tobacco. *The Plant Cell*, 9, 809–824.

Zhang, Y., Xu, S., Ding, P., Wang, D., Cheng, Y.T., He, J. et al. (2010) Control of salicylic acid synthesis and systemic acquired resistance

by two members of a plant-specific family of transcription factors. *Proceedings of the National Academy of Sciences*, 107, 18220–18225.

Zheng, X.Y., Spivey, N.W., Zeng, W., Liu, P.-P., Fu, Z.Q., Klessig, D.F. et al. (2012) Coronatine promotes *Pseudomonas syringae* virulence in plants by activating a signaling cascade that inhibits salicylic acid accumulation. *Cell Host & Microbe*, 11, 587–596.

Zhou, N., Tootle, T.L., Tsui, F., Klessig, D.F. & Glazebrook, J. (1998) PAD4 functions upstream from salicylic acid to control defense responses in *Arabidopsis*. *The Plant Cell*, 10, 1021–1030.

Zipfel, C., Robatzek, S., Navarro, L., Oakeley, E.J., Jones, J.D.G., Felix, G. et al. (2004) Bacterial disease resistance in *Arabidopsis* through flagellin perception. *Nature*, 428, 764–767.

Šimura, J., Antoniadi, I., Široká, J., Tarkowská, D., Strnad, M., Ljung, K. et al. (2018) Plant hormonomics: multiple phytohormone profiling by targeted metabolomics. *Plant Physiology*, 177, 476–489.

SUPPORTING INFORMATION

Additional supporting information can be found online in the Supporting Information section at the end of this article.

How to cite this article: Zhang, C., Atanasov, K.E., Murillo, E., Vives-Peris, V., Zhao, J., Deng, C. et al. (2023) Spermine deficiency shifts the balance between jasmonic acid and salicylic acid-mediated defence responses in *Arabidopsis*. *Plant, Cell & Environment*, 46, 3949–3970. https://doi.org/10.1111/pce.14706